



**Performance of WRF Large-Eddy Simulations in summertime CBL characteristics over the Taklimakan Desert: A Real Test Case**

Journal:	<i>Journal of Meteorological Research (JMR)</i>
Manuscript ID	ACTA-E-2018-0001.R1
Manuscript Type:	Original Article
Date Submitted by the Author:	19-Apr-2018
Complete List of Authors:	Xu, Hongxiong Wang, Minzhong Wang, Yinjun; Chinese Academy of Meteorological Sciences, State Key Laboratory of Severe Weather
Keywords:	WRF, Large Eddy Simulation, Convective Boundary Layer, Taklimakan
Speciality:	Large Eddy Simulation, Convective Boundary Layer

SCHOLARONE™  
Manuscripts

1       **Performance of WRF Large-Eddy Simulations in summertime CBL**  
2       **characteristics over the Taklimakan Desert: A Real Test Case**

3  
4  
5               Hongxiong Xu<sup>1</sup>, Minzhong Wang<sup>124</sup>, Yinjun Wang<sup>1</sup>, Wenyue Cai<sup>13</sup>  
6

7  
8  
9  
10  
11  
12  
13  
14  
15  
16  
17               1 State Key Laboratory of Severe Weather, Chinese Academy of Meteorological Sciences  
18   Beijing, China 100081

19               2 Institute of Desert Meteorology, CMA (Chinese Meteorological Administration),  
20   Urumqi, China

21               3National Climate Center, Chinese Meteorological Administration,  
22   Beijing, China 100081

23               4 Taklimakan Desert Atmospheric Environment Observation Experimental Station, Tazhong 841000,  
24   China

25  
26  
27  
28  
29

30       Submitted to **Journal of Meteorological Research**

31       January 2, 2018

32       Corresponding author:

33       Dr. Minzhong Wang

34               Institute of Desert Meteorology,  
35               CMA (Chinese Meteorological Administration),  
36               No. 46, Zhongguancun South Street, Haidian District, Beijing  
37               P. R. China, 100081

38       Email: [wangmz@idm.cn](mailto:wangmz@idm.cn)  
39               dorn1984@163.com

## Abstract

During the summer season over Taklimakan Desert, the maximum height of the CBL (convective boundary layer) can exceed 5,000 m, which appeared to play critical roles in simulating the regional circulation and weather. In this paper, we use a combination of WRF-LES (Weather Research and Forecasting Model Large-Eddy Simulation), the GPS radiosonde and eddy-covariance station to evaluate the performance of WRF-LES in the deep convective PBL case over the central Taklimakan. Results show that the model reproduces reasonably well the evolution of PBL processes. However, simulations are relative warmer and moister than those observed due to the over-predicted surface fluxes and largescale advection. Tests are further performed with multiple configurations and sensitive experiments. Sensitivity tests to Lateral Boundary Condition(LBC) showed that the model results are very sensitive to changes in time resolution and domain size of Specified LBC. It is found that larger domain size varies the distance of the area of interest from the LBC, is efficient to reduce the influences of large forecast error near the LBC. However, more frequently updated LBC is desirable to inhibit model error near the LBC. On the other hand, model error increased as the distance between the area of interest and the lateral boundaries decreased. Furthermore, comparing model results using the original surface land parameterized sensible heat flux(SH) with Noah land-surface scheme and those of sensitive experiment, it is concluded that the desert CBL is very sensitivity to SH produced by surface land scheme during summer day time. A reduction in SH can correct overestimate of the potential temperature profile. However, increasing SH significantly reduce the total time needed for CBL increase to a relative low altitude (< 3 km) at the middle and preliminary stage of the development of CBL rather than produce higher CBL at the late stage

63    Keyword: WRF, Large Eddy Simulation, Convective Boundary Layer, Taklimakan

64

65

For Review Only



## 1 Introduction

The Taklimakan Desert, **locates** at the south center of the province of Xinjiang, China, is the world's second-largest **flow desert** and has profound influences on the regional weather and climate. Because of the extreme near-surface temperatures, the Taklimakan PBL (planetary boundary layer) commonly reaches 4–6 km during boreal summer(Wang et al.), making it probably the deepest on earth. The deep PBL, which is significantly higher than that of the surrounding mountains and oases, appeared to play important roles on regional circulation and weather. In the northwest of **china**, the ability to accurately forecast in Taklimakan Desert especially the PBL processes is an important problem.

The large desert (such as Sahara, Taklimakan et al.) atmosphere is always a key component of the climate system. The surface heating from intense solar radiation leads to the development of a near-surface thermal low pressure system, commonly referred to as the heat low(Engelstaedter et al. 2015). However, despite of the vital role of the desert playing in the climate system, observations are extremely sparse, and thin data that exist are mostly from the surrounding of the desert due to the poor work and natural(Marsham et al. 2011). This fundamentally restrict the development of understanding desert and surrounding area, and leads to large discrepancies to analyses and significant biases in operational numerical weather prediction (NWP) models, given the scarcity of observation being assimilated by operational systems. The ability of these local models to simulate real-world cases is often hindered by a lack of favorable data needed to assess the performance of model results(Garcia-Carreras et al. 2015). To fill in the gaps of Taklimakan desert, the field observation experiment was held during the month of July 2016 in Tazhong, which is located

88 at center of Taklimakan, by the Institute of Desert Meteorology (IDM), Chinese  
89 Meteorological Administration (CMA), Urumqi(Liu et al. 2012; WANG et al. 2016a; Wang  
90 et al. 2016b). This will also give the opportunity to evaluate the performance of the deep PBL  
91 process in NWP models over Taklimakan.

92 On the other hand, atmospheric motions interweave small-scale, complex and multiscale  
93 nonlinear interactions. Due to the limited resolution (time and space) mesoscale atmospheric  
94 models are still unable to explicitly represent all these processes(Talbot et al. 2012). Such  
95 processes include turbulent motions, which are too small-scale to be explicitly resolved in the  
96 atmospheric model by a simplified process. Furthermore, turbulent mixing throughout the  
97 PBL can heavily impacted NWP forecasting (Shin; Hong 2011; Shin; Hong 2015).

98 One way to tackle complex turbulent flows in weather forecast models is Large eddy  
99 simulation (LES) which explicitly resolve energy-containing turbulent motions that are  
100 responsible for most of the turbulent transport(Moeng et al. 2007). It has been used  
101 intensively to examine detailed turbulence structure, to generate statistics, and to perform  
102 physical-process studies(Garcia-Carreras et al. 2015; Heinold et al. 2013; Heinold et al. 2015;  
103 Heinze et al. 2015; Sun; Xu 2009). However, most LES applications to the PBL have been  
104 limited to idealized physical conditions. Recently, some studies attempt to test LES and assess  
105 its performance in simulating real cases(Liu et al. 2011; Talbot et al. 2012). Liu et al. (2011)  
106 suggests that WRF-LES is a valuable tool for simulating real world microscale weather flows  
107 and for development of future real-time forecasting system, although further LES modeling  
108 tests, such as elucidate whether inaccurate synoptic forcing or coarse resolution, are highly  
109 recommended. Talbot et al. (2012) suggested that the ability of WRF-LES to simulate

real-world cases are hindered by a lack of favorable synoptic forcing. The initial(ICS) and lateral boundary conditions(LBCS) was found to be more critical to the LES results than subgrid-scale turbulence closures. Thus, the LBCS of can significantly alter high-resolution LES status through inflow boundaries(Rai et al. 2017).

However, most of research above on LES over desert has been limited to idealized physical conditions(Garcia-Carreras et al. 2015) or conducted real case outside Taklimakan(Liu et al. 2011; Talbot et al. 2012). The aim of this study is the attempt to applicate LES in a real deep CBL case over Taklimakan. An important aspect of the ongoing this paper is to examine assess the skillfulness of WRF-LES in relative coarse resolution (333m) over Taklimakan dessert in simulating real cases of deep desert PBL process during boreal summer events in Taklimakan. First we use a combination of WRF-LES and the GPS radiosonde and surface fluxes calculated by an eddy-covariance method taken in the central Taklimakan to evaluate the performance of WRF-LES in real case. Then we assess the potential errors related to LBC. Moreover, we aim to evaluate the relative contribution of uncertainties in surface model to the typical behavior of PBL processes by conducting the sensitivity experiments. Thus, the sensitivity of the performance to surface sensible heat flux (SH) is also studied. Section 2 gives a brief description of synoptic of the study case, and we described data and model configuration and design of numerical experiments used in this study. We presented the results of numerical simulations in Section 4. Finally, we summarize conclusions in Section 5.

## **2 Method**

### **2.1 Model configuration**

The WRF model of version 3.8.1 (Skamarock et al. 2008) is utilized here at sub-kilometer resolutions to simulate the extreme CBL event in Taklimakan desert. The model is integrated for 12h, starting from 0800 BJT (Beijing Time) 01 Jul 2016. We conducted one-way nest WRF from mesoscale down to LES-scales. All domains were 51 levels extended to 50 hPa. Height for lowest 20 levels are 1130.473, 1157.705, 1207.765, 1294.703, 1423.873, 1591.895, 1795.526, 2021.868, 2272.33, 2558.433, 2882.675, 3248.113, 3658.499, 4118.481, 4633.882, 5212.111, 5855.802, 6517.111, 7151.295, 7757.151. The model horizontal spacing is 12km 3km 1km and 0.33km for d01 d02 d03 and d04. The sizes of model grids are 411 ×321 791x651 211x201 and 403x406 respectively. Figure 1 shows the domain for all experiments except for BDY\_T3. Smaller grid sizes (205 X 208) are used in experiment BDY\_T3 to verify the effect of domain size on LES simulation.

The initialized condition and lateral boundary conditions are provided to the coarsest mesoscale simulations from NCEP Global Data Assimilation System (GDAS) Final Operational Global Analyses. The analyses are 0.25-degree by 0.25-degree grids prepared operationally every six hours and available on the surface, at 32 mandatory (and other pressure) levels from 1000 millibars to 10 millibars (National Centers for Environmental Prediction 2015).

The model physical options include the WSM5 microphysics scheme (Hong; Lim 2006), the Yonsei University (YSU) planetary boundary layer scheme (Hong; Pan 1996), the Kain–Fritsch cumulus parameterization scheme (Kain 1993; Kain 2004), RUC (Rapid Update Cycle) land-surface model (Smirnova Tatiana et al. 2000; Smirnova et al. 1997), the Rapid Radiative Transfer Model (Mlawer et al. 1997) longwave, and the Dudhia shortwave radiation scheme

(Dudhia 1989). The cumulus parameterization scheme is only applied to the d01(12km) grid domain to parameterize the convective rainfall. While, the large-eddy-simulation (LES) is only applied to d04(0.333km).

Table 1 shows the list of experiments. Experiment 1 was the control experiment, denoted as CTRL. The experiment 2 (6-hour update LBC, denoted BDY\_T2) and experiments 3(with domain sizes 205 X 208, denoted BDY\_T2) were conducted the same as CTRL with different domain sizes and LBC update frequency. In experiment 4 (denoted HFX\_%75) and 5 (denoted HFX\_%125), the SH (sensible heat flux) was reduced to 75% and 125% of that in the control experiment in the RUC land-surface scheme, to highlight the impact of SH on deep CBL at Taklimakan desert, respectively. In experiment 6 (denoted Noah), Noah land-surface model(Chen; Dudhia 2001a, 2001b) was used to replace the RUC land-surface model in CTRL experiment to discriminate the influence of different land-surface model on deep CBL.

## 2.2 Data

The model simulations are compared to the Tazhong field experiment, which was held during the whole month of July 2016 in Tazhong, by the Institute of Desert Meteorology (IDM), Chinese Meteorological Administration (CMA), Urumqi. The main station was located at 86.63° E, 39.03° N. The location is relatively flat with few hills and covered by sand combined with grass (Figure 1), and the deep PBL of our simulation was under a cloudless sky and dry environment. Instruments are described as follows:

1) surface fluxes: The eddy correlation system was a R3-50 supersonic anemometer developed by Gill Company, UK, deployed at a height of 10 m. The data acquisition

frequency was 20 Hz, and the surface sensible heat flux was calculated by the eddy-covariance method.

2) vertical profiles measured using soundings: Upper air soundings of temperature, pressure, humidity, and wind speed and direction were conducted 3-6 times per day with the GPS sounding system developed by No. 23 Institute of China Aerospace Science & Industry Corp. (CASIC23). The sounding times were 01:15, 07:15, 10:15, 13:15, 16:15 and 19:15 respectively.

### 2.3 Synoptic

Figure 2 shows the synoptic patterns at 0800 BJT 1 July 2016 at 850 700 500 and 100 hPa. There were cyclonic vortex from 850 to 500 hPa center at  $55^{\circ}$  N (Figure 2a ,b and c). Taklimakan was located east of cyclonic vortex and embedded in east–west–elongated ridge at 0800 BJT 1 July. To the southwest, influenced by the South Asia High, which was centered over the eastern Iranian Plateau, the upper air over the Taklimakan Desert was controlled by the westerly jet stream at 100hPa (Figure 2 d). The low-pressure system at low level, which is termed of heat low (Figure 3), dominated most area of southern Xinjiang and resulted in continuous high temperature over the desert. This situation favored the subsidence motion and served as a triggering mechanism for deep PBL in the region in the coming 2–3 days (not show).

## 3 Results

### 3.1 Validation of the deep CBL structure

Time series of surface variables at Tazhong station from CTRL simulation for 01 July 2016 are presented in Figure 4a, b. Results show that discrepancies of thermodynamic surface

variables (the surface temperature, sensible and latent fluxes) between model and observation are large during simulation. The SH (surface sensible heat flux) is far less in observation (maximum:  $243 \text{ W m}^{-2}$ ) relative to model (maximum:  $613 \text{ W m}^{-2}$ ). This represents SH from WRF simulation is 2.5 times than that of observation when both of which reach its maximum. On the other hand, model shows a significant cold bias for the surface temperature. The surface temperature is much higher in observation (maximum:  $70^\circ\text{C}$ ) relative to model (maximum:  $50^\circ\text{C}$ ). To further verification the surface variables, RMSE (root mean squared error) and BIAS (mean bias) are calculated including integration hours from 3 to 12 h for Tazhong station in Table 2. As mentioned earlier, model show yields significantly overestimate of SH (RMSE  $263.636 \text{ W/m}^2$ , BIAS:  $250.14 \text{ W/m}^2$ ) and dramatically underestimated of surface temperature (RMSE  $14.65^\circ\text{C}$ , BIAS:  $-13.37^\circ\text{C}$ ).

Two possible reasons result in model SH far above that of observation: (1) The mismatches of land-use between the model and the observation. WRF use land-use categories to assign certain static parameters and initial values to each grid cell, for example, albedo, surface roughness, and so on (Schicker et al. 2016). However, As in Figure 1c, the EC station is surround by mixing land of grass and sand. The complex underlying surface may not be adequately reproduced by model and can have an impact on the overestimate of SH in this case. (2) It is should be noted that the SH and LH (latent heat flux) based on eddy correlation might be underestimated (LeMone et al. 2013). Researchers found that if the other two terms in the budget—net radiation and flux into the soil were accurate, used data for the whole experiment to find the  $H + LE$  for Tazhong station are equal to an average of 75% of what would be required for balancing the surface energy budget.

Despite the large differences on surface, near-surface variables (2m temperature, relative humidity and 10m wind speed, Figure 4 e f g) are closer to measurements than those from surface, their values are relatively higher than those observed. The time series evolution of 2m temperatures nearly follow those of the observations (RMSE:1.66, BIAS:1.61); but model produce warmer surfaces by about 3 K at the beginning of model integration, and 1K when model and observation both reach their maximum temperature, respectively.

Results indicate that, model-produced near-surface relative humidity is close to observations at initial time (Figure 4 f). However, the humidity from the model keeps increasing at the first few hours of model integration, when observations decrease. After 3 hours' spin-up, the model reproduces reasonably well the evolution of humidity, in agreement with observation (RMSE:1.22), but their values are relative higher than those observed(BIAS:1.11).

One reason for this discrepancy is the overestimate of soil moisture during simulation. Soil moisture can severely impact near-surface humidity. The overestimate of the soil moisture contents in the initial condition of the model, which are only offered to the model at initial time, may result in considerable differences in near-surface layer humidity (Talbot et al. 2012). In the present simulations, model results are reported to produce grossly overestimate soil moisture. At the model initialization for the CTRL simulation, EC station at Tazhong station indicated a value of the 5-cm-deep soil moisture of  $0.230 \text{ m}^3/\text{m}^3$ , while the model initial value is  $0.6 \text{ m}^3/\text{m}^3$  (Figure 4 d). This large overestimate of soil moisture results in LH (Figure 4 b, f) from the model continue to increase. As a result, near-surface of model is far moister than that of observation at the first few hours of model integration. An interesting



result to note is that the model simulation has the abilities to correct some of the bias due to the initial condition of the surface; The results from CTRL experiment are closer to observation after 3 hours' spin-up.

The model simulated potential temperature are compared to GPS sounding measurements at Tazhong during 0800~2000 BJT 01JULY2016 in Figure 5 (solid lines). One should note that radio-sounder floating about 7 Km away from Tazhong, when radio-sounder reach 6 Km height. Thus, for comparison, the profiles of model simulations are averaged station in a radius of 3.5 Km. At 0800 BJT, when the model is initialized, the nocturnal inversion reaches 300m (not shown). By 1100 BJT, this inversion is eroded in the model in agreement with observations, and both reaching about 300m at 1100 BJT (Figure 5 a). However, the simulated CBL grows faster in the morning due to larger SH than observation, reaching 3500m (3000m in the observations) at 1400 BJT (Figure 5 b). At 1700 BJT (Figure 5 c), the simulated and observed CBL heights exceed 4000m and 5000m respectively. This indicates that the simulated CBL grows more slowly in the afternoon than measurement. Compared to measurements, the model is initially cooler with faster heating rate in the morning. As a result, model is warmer than measurements in the afternoon. Eventually, model agrees with observations at the end of the day. One possible minor reason is the differences of potential temperature lapse rate above the top of mixing layer between observation and simulation. Simulated stronger inversion layer restrain the development of CBL, which will be discussed below.

Moreover, in terms of CBL temperatures, the model initially simulates a cooler and drier CBL than that observed, at 1100 BJT 01 JUL (Figure 5a). Compared to the observed potential

temperature profile, the CBL seems to appear earlier in model forecasts result based on obvious warming in surface layer. One should note that RL (residual layer) may play a key role in the deep PBL at Taklimakan desert. At 1100 BJT, when the CBLH was about 300 m in observation as show above, potential temperature in the were about 317 in PBL and 320 K in RL, respectively. When the potential temperature in CBL increased to the value in RL (320 K), the CBL merged with the RL, and the height of PBL reach 3000m in the observations at 1400 BJT. These results are in good agreement with Han et al. (2012). By analysis of observation of a CBL in the Badanjilin region, they found a rapid development process of CBL after 1200 LST, which appeared to be a jump of CBLH when the inversion layer vanished.

When the SH reaches its maximum at 1400 BJT (Figure 5b), potential temperature profile is closer to measurements than at initial time, and their values are higher than those observed. By 2000 BJT (Figure 5d), CBLH in the model reaches its maximum value, which is consistent with observation, despite of approximately 0.4K cooler on the lower levels(<2.5Km). As mentioned, one cause of the higher temperatures produced with model would be the large difference in the surface heat fluxes. It was concluded that the surface sensible heat flux from the land surface parameterization is the crucial factor affecting the CBL process during summer day time. Differences in surface SH would create differences in the vertical development of the PBL. Thus, the large surface SH difference between the model and observation may lead to differences in CBL growth during daytime and in its peak depth during the simulation. Fortunately, one can artificially modify the surface SH computed by surface-land model, which

controls the calculation of surface fluxes. Sensitive simulations will be realized and discussed in next section.

Figure 5 also shows Vertical profiles of vapor mixing ratio (dash lines) at Tazhong station. The simulated profiles with lower RL are much drier than observation from 1500 to 3500m at 1100 BJT. The vertical mixing results in the uniform structure of vapor mixing ratio within CBL, so the differences between simulated and observational profiles are reduced remarkably when CBL reach above 4000m at 1400 BJT. Differences are generally less than 1g/Kg at 1100 BJT reaching a maximum of 0.3g/Kg at 1400 BJT. However, measured PBL moisture shows an inverse layer at lower PBL( $\leq 2000$ m) range from 2.8 to 3.6 g/Kg, which is not captured by model. Furthermore, as the convective boundary layer grows, the inversion moisture structure below 3000m develops to and maintains below 3000m during 1400~2000 BJT. By the end of the day, the model-simulated CBL humidity show moister than observation, because model cannot reproduce the inverse moisture layer within CBL.

Inverse humidity may be caused by the joint of the heterogeneous humidity Pattern and Large-scale advection over the underlying surface. For instance, interaction of oasis with desert environment may resulted in the inverse humidity layer in desert PBL. Thus, one possible reason for the discrepancy between model and observation caused by the error in land-use type. The USGS land-use in ARW-WRF is based on AVHRR (Advanced Very High Resolution Radiometer) 1km resolution satellite data during 1992-1993. For our case, this land-use data may be outdated in Taklimakan. Besides such changes, misclassifications are found in the USGS land-use data, the default land-use dataset in WRF(Schicker et al. 2016). This is also confirmed by the discrepancies of land-use between simulation and measured at

the Tazhong station in the previous figure. Large-scale advection of dry air can affect the profile of moisture. Moisture will also be variable in the horizontal, so advection at the low level could contribute to the dry at bottom and moisture at the upper of PBL between 1100 and 2000 BJT at the bottom of the PBL.

The mismatch between the model and the observations in terms of moisture that is present means that the effect of land-use type and Large-scale advection needs to be quantified and that more detailed data of Taklimakan (land and atmosphere) might be necessary to realize a more realistic performance. Extra care should also be taken with sparse and the limited data in the periphery of the Taklimakan (ter Maat et al. 2012).

### 3.2 Sensitive to Lateral Boundary Condition(LBC)

After verifying the details of the LES simulations, we assess the sensitivity of the LES simulations to time resolution and domain size of Specified LBC. For one-way nest, Specified LBC is obtained from coarser model simulation. The analysis and all forecast times from a previously-run larger-area model simulation are used to specify the LBC. The primary cause of differences in PBL structure was diagnosed as differences in domain size and frequency provided by the coarser resolution. The aim is to assess the sensitivity of the finer large-eddy simulations to time frequency and domain size of Specified LBC forcing by larger-area model simulation; Details of the three simulations (CTRL, BDY\_T2 and BDY\_T3) are given in section 2.

Figure 5 compare the profiles of the simulated potential temperature and vapor mixing ratio profiles from LBC sensitivity experiments and observation. Results indicate that, there is a distinct relationship between LBC and CBL development. All model-produced profiles are

nearly the same at initial time (not show). However, the comparison results reveal that discrepancies among different experiments are large for CBL. The results indicate that larger domain size and more time frequency LBC leads to a warmer and drier PBL, but a cooler and moister free troposphere. Such sensitivity is monotonic with respect to LBC (Figure 5). Furthermore, in the next three hours, the differences between the sensitive experiments keep increasing with time (Figure 5 a, b). The potential temperature profiles within CBL become divergence at 1100 BJT. However, the results show more convergence at afternoon as CBL continues to grow (Figure 5 c). Finally, largest discrepancies are found by end of the day (Figure 5 d) where the model CBL potential temperature is warmer by up to about 0.7K and 0.9K in BDY\_T2 and BDY\_T1 respectively, compared to measurements.

Figure 6 shows cross sections along  $39.03^{\circ}\text{N}$  of horizontal winds, superposed with theta and vapor mixing ratio. Overall, the lower frequently updated LBC is desirable to cold zone near the LBC, which results in cold advection of the temperature and moisture to the area of interest (Figure 6 b, c). Larger domain size, which varies the distance of the area of interest from the LBC, is efficient to reduce the influences of large forecast error near the LBC to the area of interest (CMP Figure 6 a, c). The results suggest that the model results are sensitive to changes in time resolution and domain size of Specified LBC. The mismatch among sensitive experiments is present means that the effect of LBC needs to be quantified to realize a more realistic performance in the sub-kilometer simulations.

To further examine the impact of LBCS on the turbulence of deep Taklimakan desert CBL, the instantaneous vertical velocity fields for the horizontal are displayed in . By 1400 BJT, the convection of CTRL simulation obviously intensified under strong surface heating

(Xu et al. 2018). Thus, the maximum vertical velocity reaches 9 m/s and the depth of mixed layer grows to about 4.3 km (a). The distances between the boundary layer rolls correspondingly increase to about 12 km and the height of the peak updraughts is raised to just under 4 km. The cellular shape of updraughts and downdraughts characteristic of boundary layer rolls is obvious in the horizontal view with the strength of convection. BDY\_T2 and BDY\_T3 experiments (b, c) both reproduce motions with much weaker maximum and minimum values at boundary of domain. In BDY\_T3 experiment, Tazhong station at center of the model has been directly influenced by the inflow cold advection produced by low frequency LBCS and results in much weaker maximum and minimum value of  $w$  (about 6 m/s). However, despite the underestimate of potential temperature, the  $w$  fields for BDY\_T2 experiment look similar to the CTRL  $w$  in plain view, and the horizontal extent of the updrafts/downdrafts agrees with the CTRL as can be inferred from . To further examine vertical structure of desert CBL, vertical cross-sections along Tazhong station ( $39^{\circ}\text{N}$ ) of  $w$  are presented in Figure 8. Wide and regularly spaced updrafts along A1- A2 split into the stronger and more irregular motions in CTRL and BDY\_T2. The updrafts are much weaker in the BDY\_T3 experiment, as can be seen from Figure 8 c. Peak updrafts on BDY\_T3 are about 4 m/s much weaker than on CTRL (9 m/s) and BDY\_T2 (8 m/s). For BDY\_T2 and BDY\_T3, the distant of the inflow boundary is wider, and the intensity of the convection is weaker at the boundary. Compared with BDY\_T2, the horizontal distribution of vertical velocity at Tazhong station in BDY\_T3 experiments is much weaker.

### 3.3 Simulations with different surface sensible heat flux (SH) and surface-land models

The import cause of differences in PBL structure was diagnosed above as differences in SH predicted by the surface-land schemes. The SH is one of the key factor affecting the CBLH during summer day time. Thus, the difference between model and observation may lead to differences in PBL growth during daytime; To further confirm whether this indeed occurs, three additional sensitive simulations were realized based on the CTRL experiment. For Noah experiment Noah land-surface model is used to replace RUC land-surface model in CTRL experiment, and for HFX-125%, HFX -75% SH is %125 and %75 that of CTRL (HFX -100%) experiment, while the other parameters remain the same.

The results from Figure 10 and Table 2 showed that HFX-75% successively improved the simulation of SH with RMSE:151.12, compared that of 263.64, 357.11 in CTRL and HFX-125%. Of interesting is that experiment with Noah surface-land yielded the best performance among all of the cases in SH, surface temperature and air temperature. However, Noah surface-land model show large discrepancies with observation in Soil moisture, and results in dramatically overestimate of LH and relative humidity compared to CTRL.

Further examining potential temperature and vapor mixing ratio (Figure 9) indicate that with smaller SH leads to a cooler, moister lower PBL and a warmer, drier free atmosphere. Such sensitivity is monotonic with respect to SH. Overall, the CBL structure from the HFX-75% and Noah experiments match the GPS measurements better than the CTRL (HFX-100%) simulations. Potential temperature profiles from CTRL (HFX-100%) and HFX-125% are consistently warmer than the observation by about 0.4 and 0.5 K respectively, while results from HFX-75% and Noah are within about 0.2K at 1400 BJT (Figure 9 b). The results suggest that the model results are sensitive to changes SH from land-surface model.

However, simulations converge at the end of the day, but remain differences at 2000 BJT (Figure 9 d). HFX-75% and Noah with weaker surface sensible heat flux can still produce the deep CBL nearly the same as CTRL and HFX-125%. This indicates that SH may not the dominant factor for the deep CBL over the Taklimakan desert.

Results of simulations on desert PBL in the morning agree with the previous studies of sensitivities land-surface model for other areas (Hu et al. 2010; Zhang et al. 2017). However, during 1700~2000 BJT 01July (Figure 9b, d), all experiments produce nearly the same CBLH and moisture in agreement with observation in the PBL. The effects of SH on the evolution of Taklimakan PBL structures during this period are needed to be further examined and discussed. So, the question is: why are simulations insensitive to land-surface process by the end of the day? As in Stull (1988), the development of CBL is mainly influenced by the effect of thermodynamic and turbulent entrainment without considering large scale factors such as large scale advection or subsidence. Besides the surface sensible heat, the intensity of entrainment process determines the increasing rate of CBL. Thus, the entrainment rate  $w_e$  is a valuable indicator for the development of PBL structure.

The rate of growth of the convective boundary layer is mainly determined by the entrainment rate  $w_e$  at the inversion layer without considering large scale vertical motion.  $w_e$  usually has a positive correlation with heat flux amount at the inversion layer  $\overline{(w'\theta_v')_h}$ , and large LES experiments show  $\overline{(w'\theta_v')_h}$  is about 0.2 times the surface flux of buoyancy  $\overline{(w'\theta_0')}$ . During the period from 1100 to 1400 BJT, larger SH is obviously correlated with stronger turbulent entrainment and warmer air from free atmosphere (FA) entraining into ML. As a result, CBL develop rapidly and is warm too fast in the early simulation phase due to the



obviously increasing temperature and strong vertical mixing in model. Of interesting is that reduction in SH reproduces better desert PBL evolution in the early simulation phase, as SH-75% and Noah produce the smallest simulation errors in both temperature and moisture. However, one should note that CBLH and potential temperature for SH-75% and Noah have reached above 5000 m and 323.2 K respectively at 1700 BJT (Figure 9 a). For the rest of the day, the increase rate of CBL height slows down due to the deep CBL(>5000m) which require more heat for the growth of PBL depth; Moreover,  $w_e$  decrease with increasing inversion intensity, which inhibits the mixing and entrainment processes. These two factors obviously limit the growth of CBL when CBLH is over 5000 m in this deep desert CBL case. Therefore, increasing SH from 75% to 125% significantly reduce the total time needed for CBL increase to a relative low altitude (< 5 km) at the middle and preliminary stage of the development of CBL rather than produce higher CBL at the late stage. When height of CBL over Taklimakan desert exceeds 5000 m, it might not change with proportion to SH fluxes (Figure 9 d). As a result, PBL of WRF simulations are basically the same, and not sensitive to SH fluxes by the end of the day.

#### 4 Summary

This paper assesses the performance of the Weather Research and Forecasting Model (WRF) Large-Eddy Simulations(LES) in deep convective PBL case over Taklimakan Desert. Tests are performed with multiple configurations and sensitive experiments. Sensitivity tests to Lateral Boundary Condition(LBC) showed that the model results are sensitive to changes in time resolution and domain size of Specified LBC. It is found that larger domain size varies the distance of the area of interest from the LBC, is efficient to reduce the influences of large

forecast error near the LBC.

Consequently, with the configuration used in this study, the model reproduces reasonably well the evolution of PBL processes. The model shows discrepancies between the main CBL characteristics in the morning including the thermal and moisture structure. The model simulates the relatively colder and drier morning CBL well, underestimating it by up to 1.5K near-surface layer at Tazhong station. In the case of the underestimation of moisture by only up to 1 g/kg in the near-surface layer. The overestimation of CBL profile may be caused by discrepancy between model and measurement initially. This indicates that the results are sensitive to the model initial conditions. An interesting result to note is that the model simulation seems to be able to correct some of the bias due to the initial condition. In the afternoon, the model correctly reproduce the thermal structure, but simulations are relative warmer and moister than those observed. Potential temperature profile at CBL appears warmer by up to about 0.4K compared to the observations. While the model overestimates the afternoon moisture seriously, it mainly overestimates vapor mixing ratio by about 1 to 2 g/Kg in the CBL. Largest discrepancies are found in 0~3Km where the model vapor is twice as moist (up to about 3g/Kg above AGL) as observed.

Furthermore, three additional sensitive simulations were realized to further confirm whether large differences of SH lead to differences in ABL growth during daytime, based on the CTRL experiment. The results suggest that the model results are sensitive to changes SH and different land-surface models. The large difference between the model and observation may lead to differences in CBL growth during daytime. From these results, it was concluded the surface sensible heat flux is an important factor affecting the CBL depth over

Taklimakan during summer day time. However, its peak depth during the simulation show less sensitive to SH because of decreasing  $w_e$  by the end of the day.

The future work aimed to study several other deep CBL cases over Taklimakan to summarize their common features. Furthermore, we hope to utilize high resolution model and observation to describe the fine characteristics of a typical deep Taklimakan CBL particularly the turbulent and vertical mixing and its impact on regional weather forecast. This research is aimed to improve the understanding of deep CBL over Taklimakan and its influence on regional weather and climate.

#### **Conflict of Interests**

The author declares that there is no conflict of interests regarding the publication of this paper.

#### **Acknowledgments**

This study is supported by the National Natural Science Foundation of China (Grant no. 41575008 and 41775030). The author would like to thank all the reviewers and editors for their professional advice to improve the paper.

477 Captions:

478 Figure 1 Simulation domains used in ARW model with terrain height (shaded, units:m); (b) land  
479 use categories for domain D03 and D04.

480 Figure 2 Horizontal distribution of geopotential height (solid, units: dagpm), wind speed (shaded,  
481 units: knot), and wind barbs from the NCEP FNL analysis at 0800 BJT 1 Jul 2016 at (a)  
482 850 hPa, (c) 700 hPa, (e) 500 hPa, and (d) 100hPa.

483 Figure 3 NCEP FNL 700hPa potential temperature (colors) and mean sea level pressure (white  
484 lines) at 0800 BJT 1 Jul 2016. The black dot shows the location of Tazhong station at  
485 Xingjiang province.

486 Figure 4 Time series of simulated surface variables from innermost domain of simulations  
487 and surface observations at Tazhong station ( $83.63^{\circ}$  E,  $39.03^{\circ}$  N) initial at 0800  
488 BJT 01July 2016 (a) sensible heat flux ( $\text{W/m}^2$ ), (b) latent heat flux( $\text{W/m}^2$ ), (c) 2-m  
489 temperature ( $^{\circ}\text{C}$ ), (d) surface temperature ( $^{\circ}\text{C}$ ), (e) 2-m Relative Humidity(%) and (f)  
490 10-m wind speed (m/s ) with corresponding observations.

491 Figure 5 Vertical profiles of potential temperature (solid line, units: K) and vapor mixing  
492 ratio(dash line, units: g/Kg)from innermost domain of simulations and observation of  
493 GPS sounding at Tazhong station ( $83.63^{\circ}$  E,  $39.03^{\circ}$  N) at (a)1100 (b) 1400 (c)  
494 1700 (d) 2000 BJT 01 Jul2016.

495 Figure 6 cross sections along  $39.03^{\circ}\text{N}$  of horizontal winds (barbs, units: m/s), at intervals of 5 m/s,  
496 superposed with theta (shaded, units: K) and vapor mixing ratio(contour, units: g/Kg), from (a)  
497 BDY\_T1, (c) BDY\_T2, (e) BDY\_T3 experiments at1400 BJT 01JUL2016, (b), (d), (f) are the  
498 same as (a), (c), (e), but for 2000 BJT 01JUL2016.

499 Figure 7 Instantaneous vertical velocity fields (shading: m/s) at 3000 m for (a) BDY\_T1 (CTRL), (b)  
500 BDY\_T2, (c) BDY\_T3, and (d) Noah at 1400 BJT, 1 July 2016.

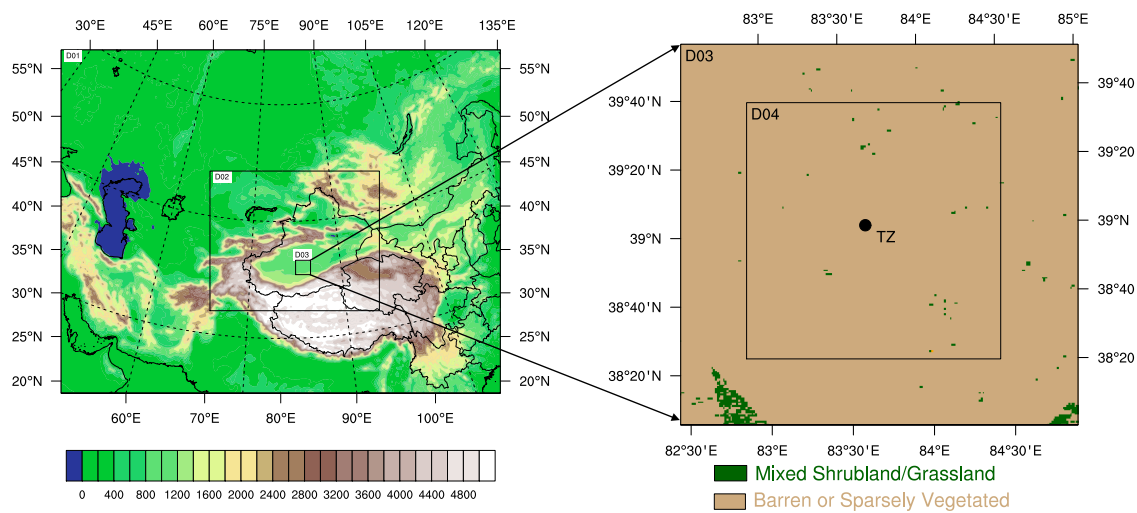
501 Figure 8 Vertical cross-section of instantaneous vertical velocity fields (shading: m/s) along  
502 A1-A2 in for for (a) BDY\_T1 (CTRL), (b) BDY\_T2, (c) BDY\_T3, and (d) Noah at 1400 BJT,  
503 1 July 2016.

504 Figure 9 The same as Figure 5, but for SH flux sensitive and Noah land-surface experiment.

505 Figure 10 The same as Figure 4, but for SH flux sensitive and Noah land-surface experiment.

506

507



508

509

(a)

(b)



510

511

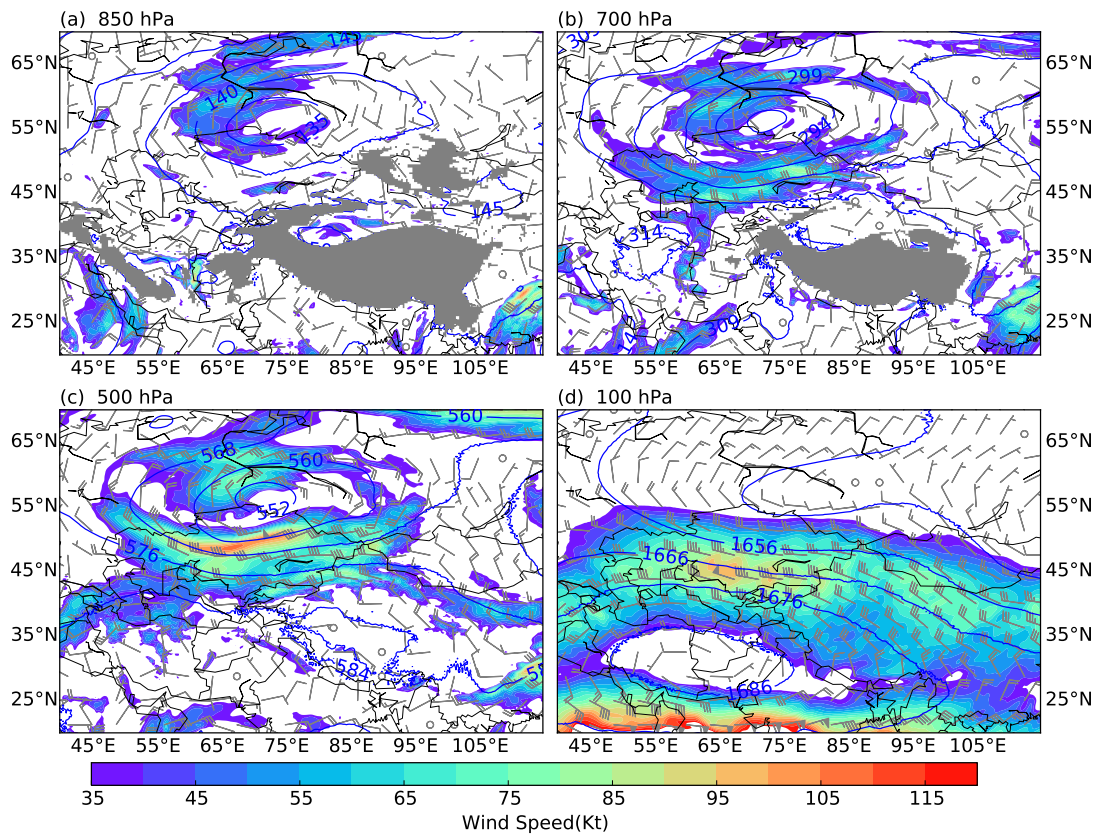
(c)

512 Figure 1 Simulation domains used in ARW model with terrain height (shaded, units:m); (b)

513 land use categories for domain D03 and D04; (c) photograph of Tazhong station

514

515



516

517 Figure 2 Horizontal distribution of geopotential height (solid, units: dagpm), wind speed  
 518 (shaded, units: knot), and wind barbs from the NCEP FNL analysis at 0800 BJT 1 Jul 2016 at  
 519 (a) 850 hPa, (c) 700 hPa, (e) 500 hPa, and (d) 100hPa.

520

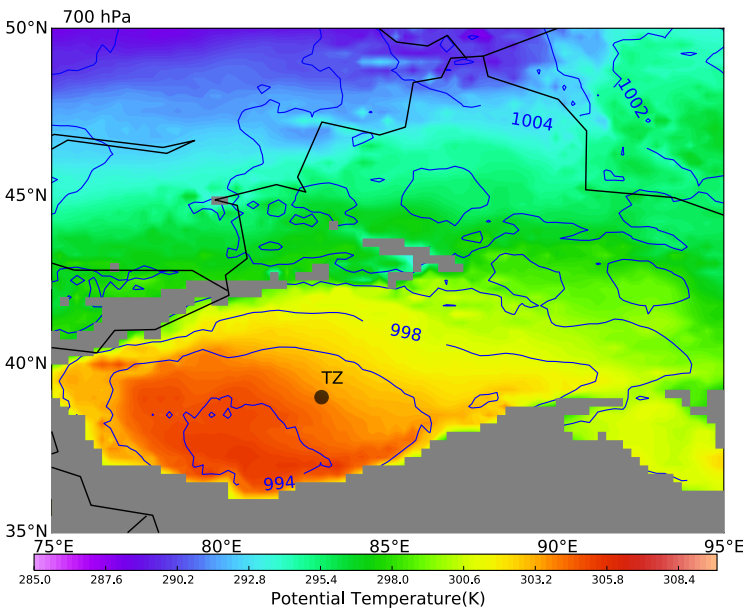


Figure 3 NCEP FNL 700hPa potential temperature (colors) and mean sea level pressure (white lines) at 0800 BJT 1 Jul 2016. The black dot shows the location of Tazhong station at Xingjiang province.



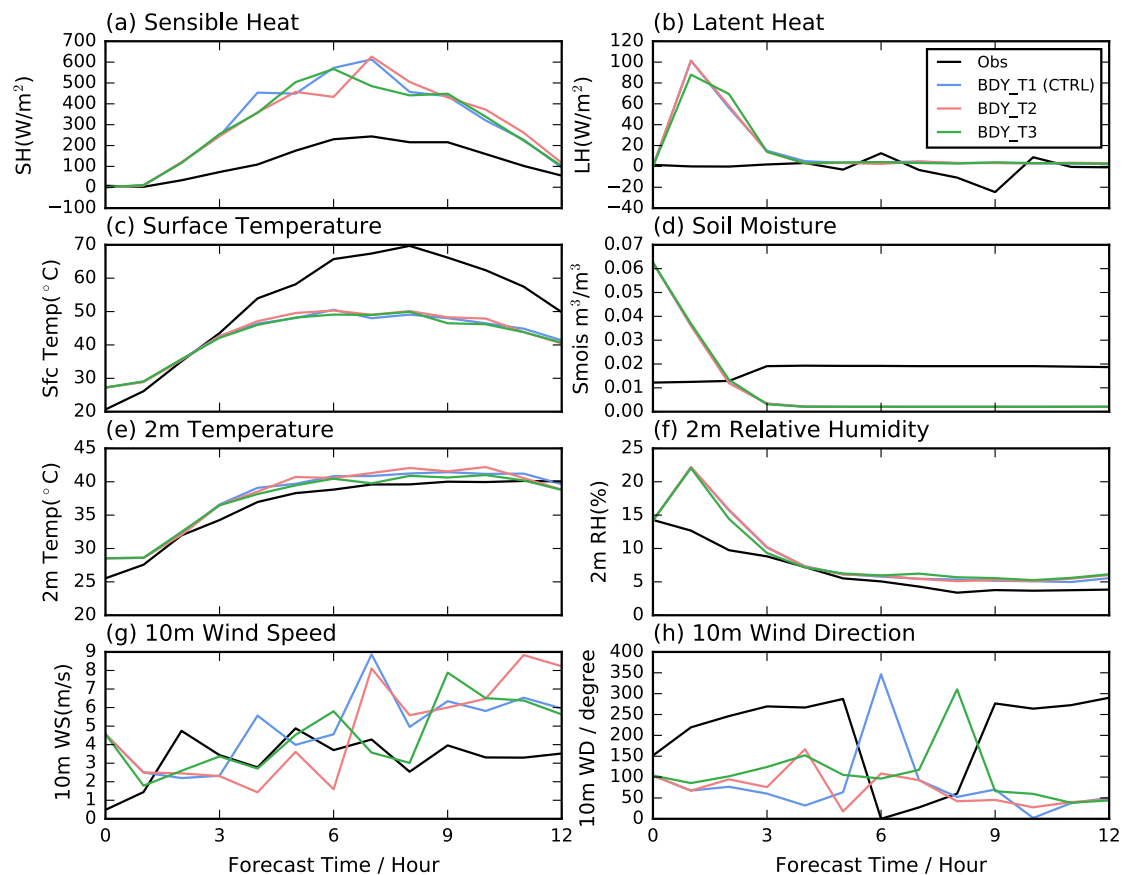


Figure 4 Time series of simulated surface variables from innermost domain of simulations and surface observations at Tazhong station (83.63° E, 39.03° N) initial at 0800 BJT 01July 2016 (a) sensible heat flux ( $W/m^2$ ), (b) latent heat flux( $W/m^2$ ), (c) 2-m temperature ( $^{\circ}C$ ), (d) surface temperature ( $^{\circ}C$ ), (e) 2-m Relative Humidity(%) and (f) 10-m wind speed ( $m/s$ ) with corresponding observations.

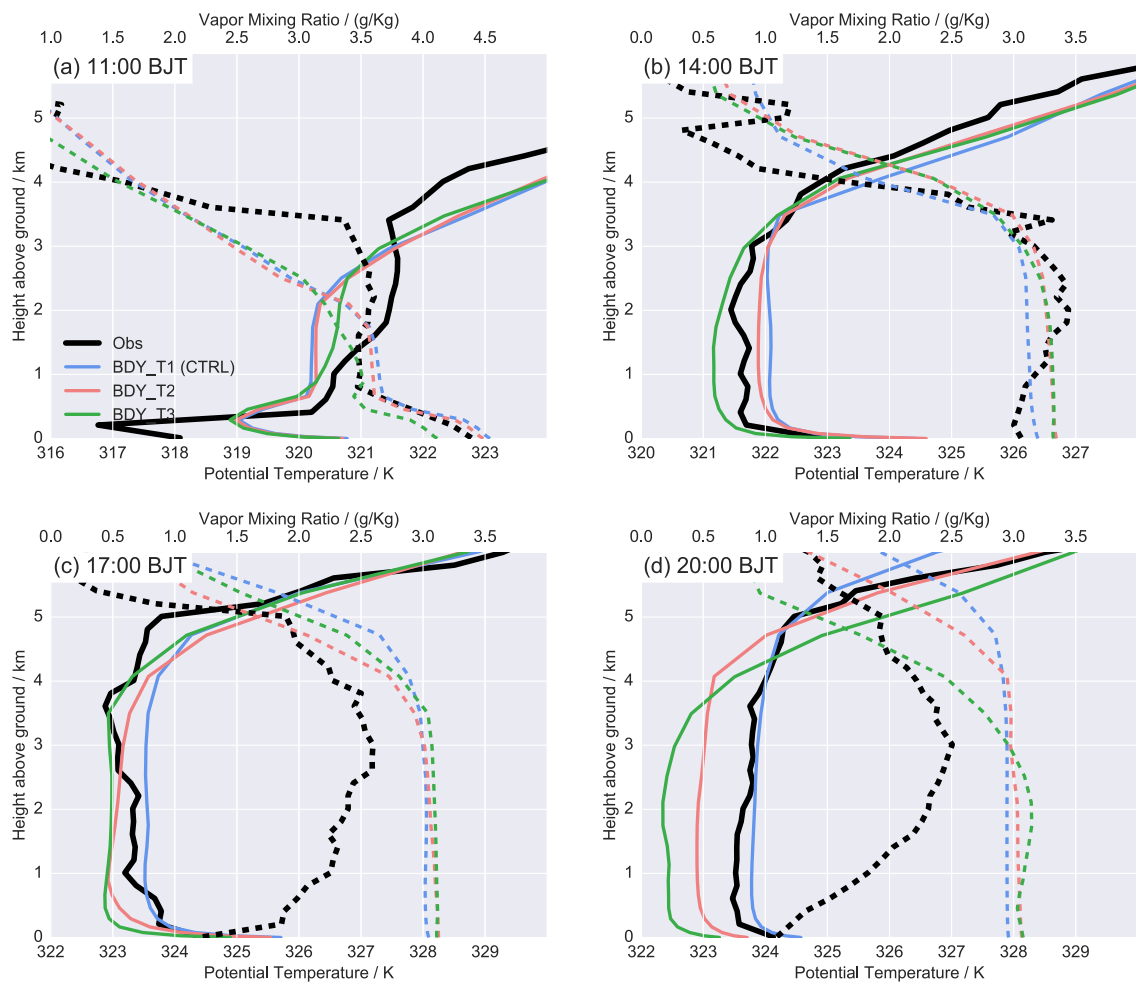


Figure 5 Vertical profiles of potential temperature (solid line, units: K) and vapor mixing ratio(dash line, units: g/Kg)from innermost domain of simulations and observation of GPS sounding at Tazhong station (83.63° E, 39.03° N) at (a)1100 (b) 1400 (c) 1700 (d) 2000 BJT 01 Jul2016. The profile of model output are averaged in a radius of 3.5km.

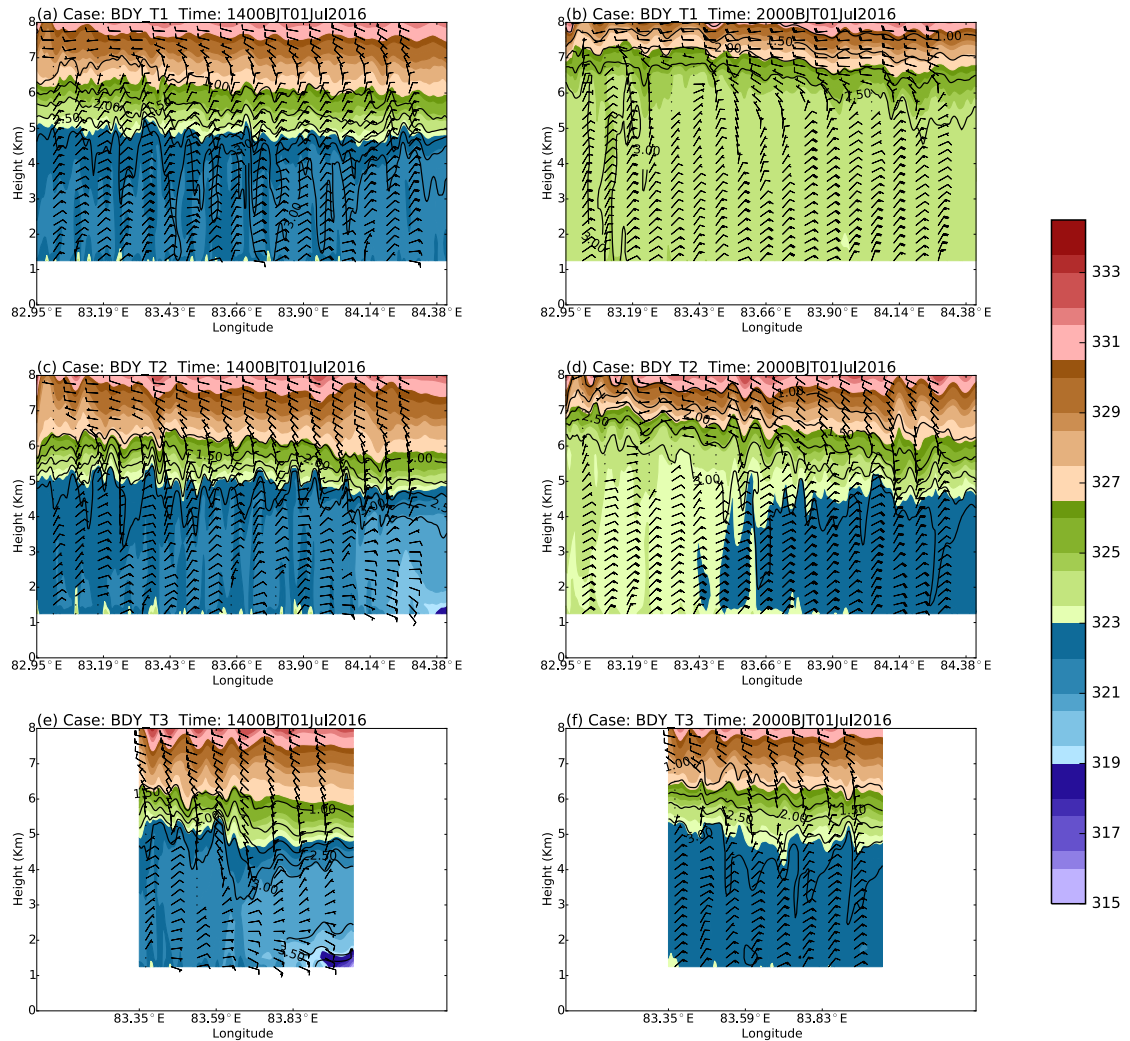
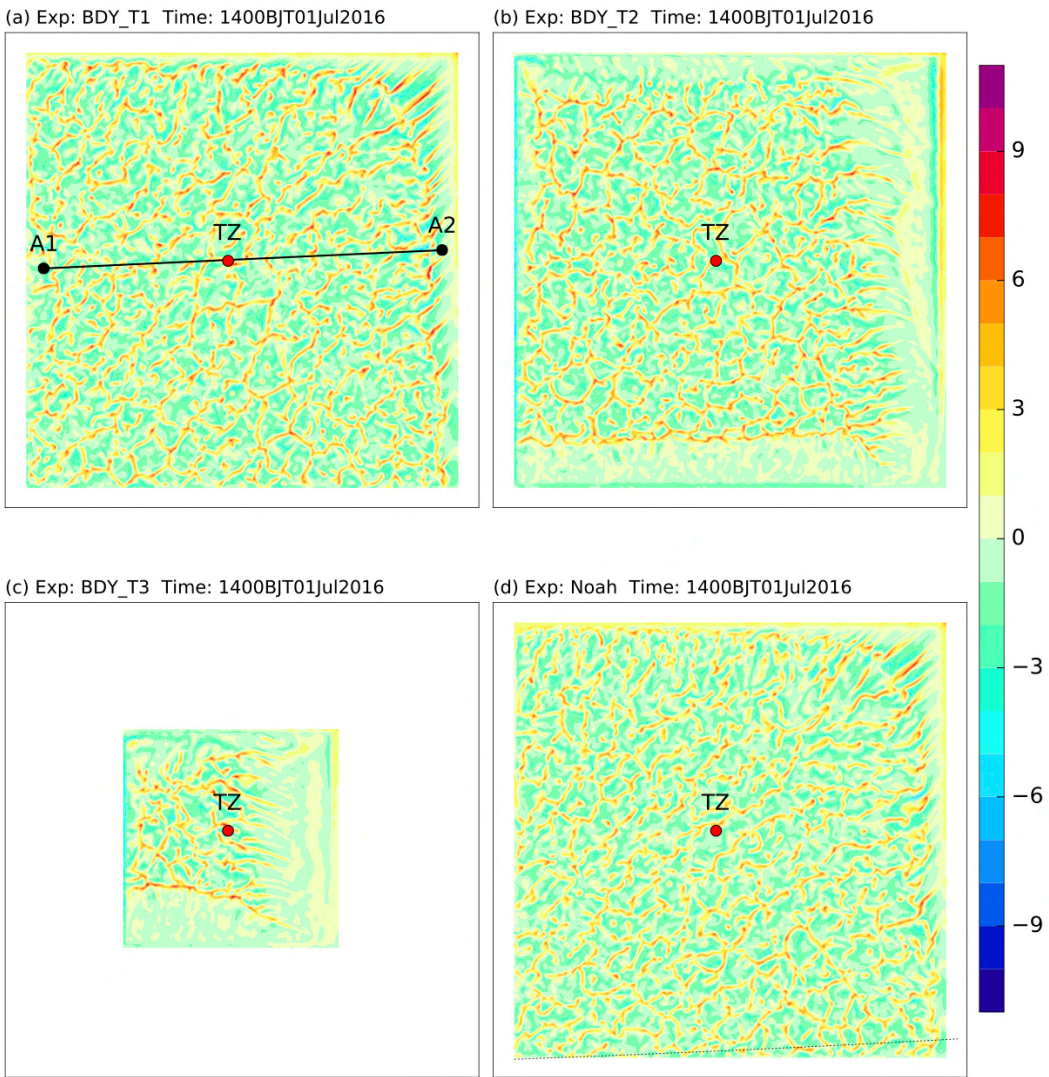


Figure 6 cross sections along 39.03°N of horizontal winds (barbs, units: m/s), at intervals of 5 m/s, superposed with theta (shaded, units: K) and vapor mixing ratio (contour, units: g/Kg), from (a) BDY\_T1, (c) BDY\_T2, (e) BDY\_T3 experiments at 1400 BJT 01JUL2016, (b), (d), (f) are the same as (a), (c), (e), but for 2000 BJT 01JUL2016.

544



545

546 Figure 7 Instantaneous vertical velocity fields (shading: m/s) at 3000 m for (a) BDY\_T1 (CTRL), (b)  
547 BDY\_T2, (c) BDY\_T3, and (d) Noah at 1400 BJT, 1 July 2016.

548

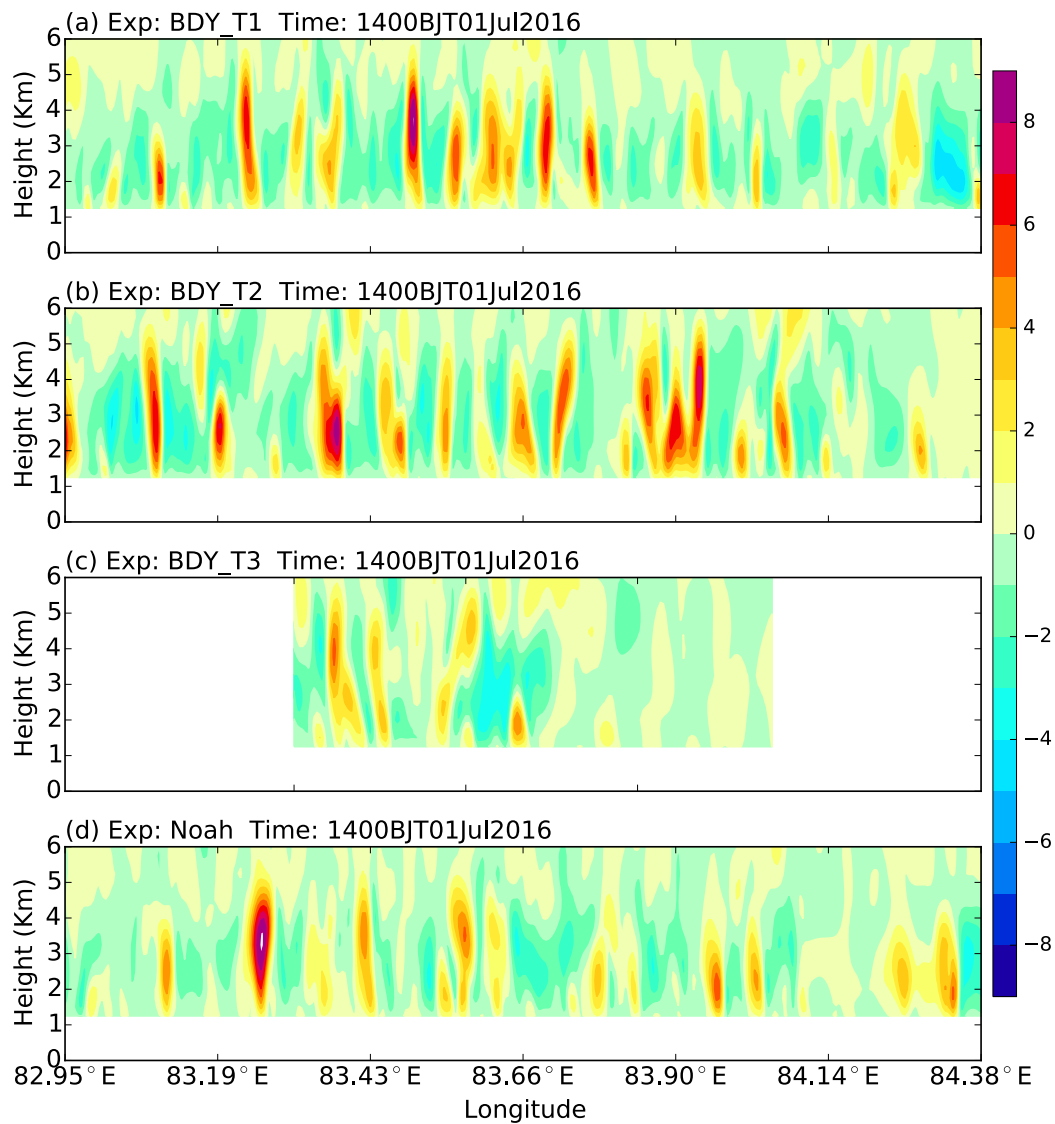
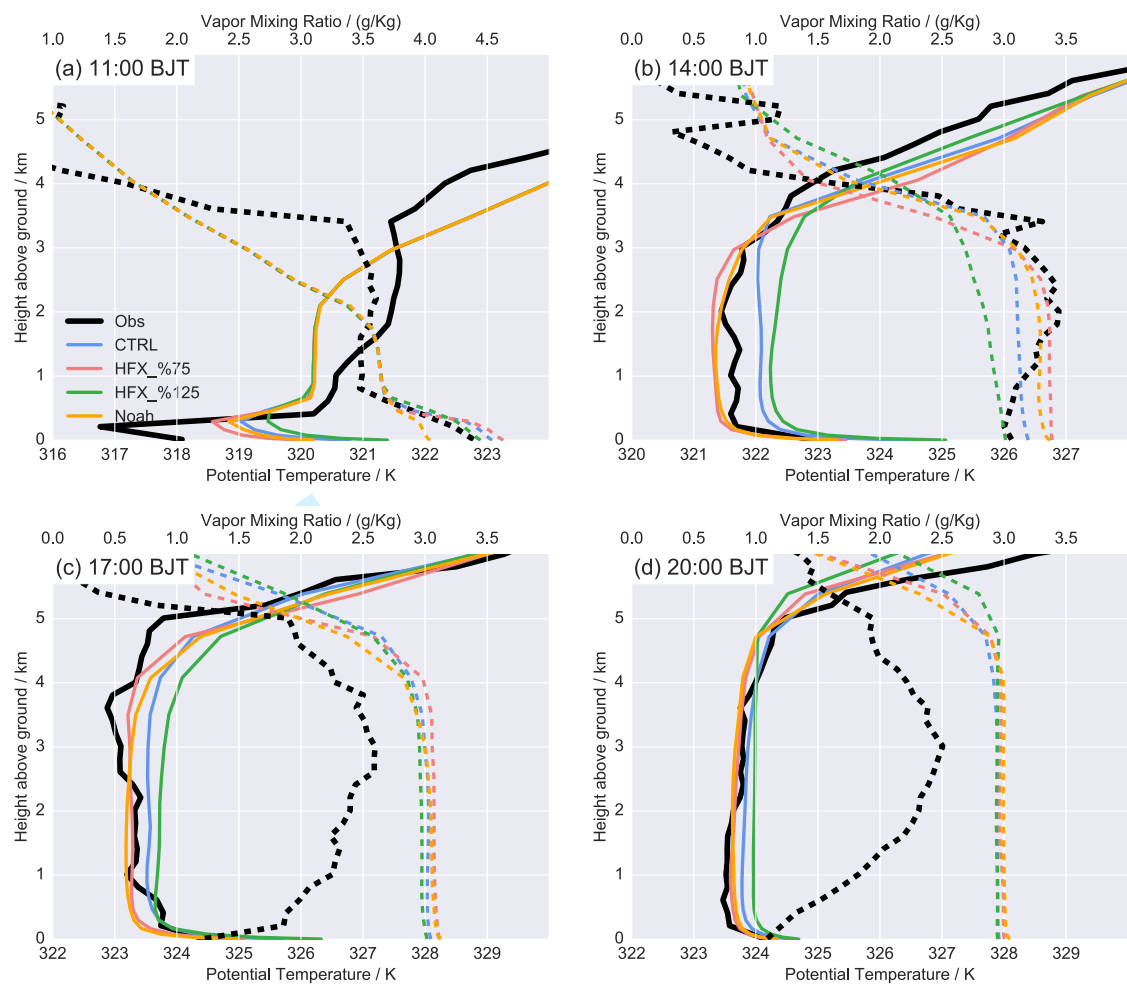


Figure 8 Vertical cross-section of instantaneous vertical velocity fields (shading: m/s) along A1-A2 in for for (a) BDY\_T1 (CTRL), (b) BDY\_T2, (c) BDY\_T3, and (d) Noah at 1400 BJT, 1 July 2016.

555



556

557

558

Figure 9 The same as Figure 5, but for SH flux sensitive and Noah land-surface experiment



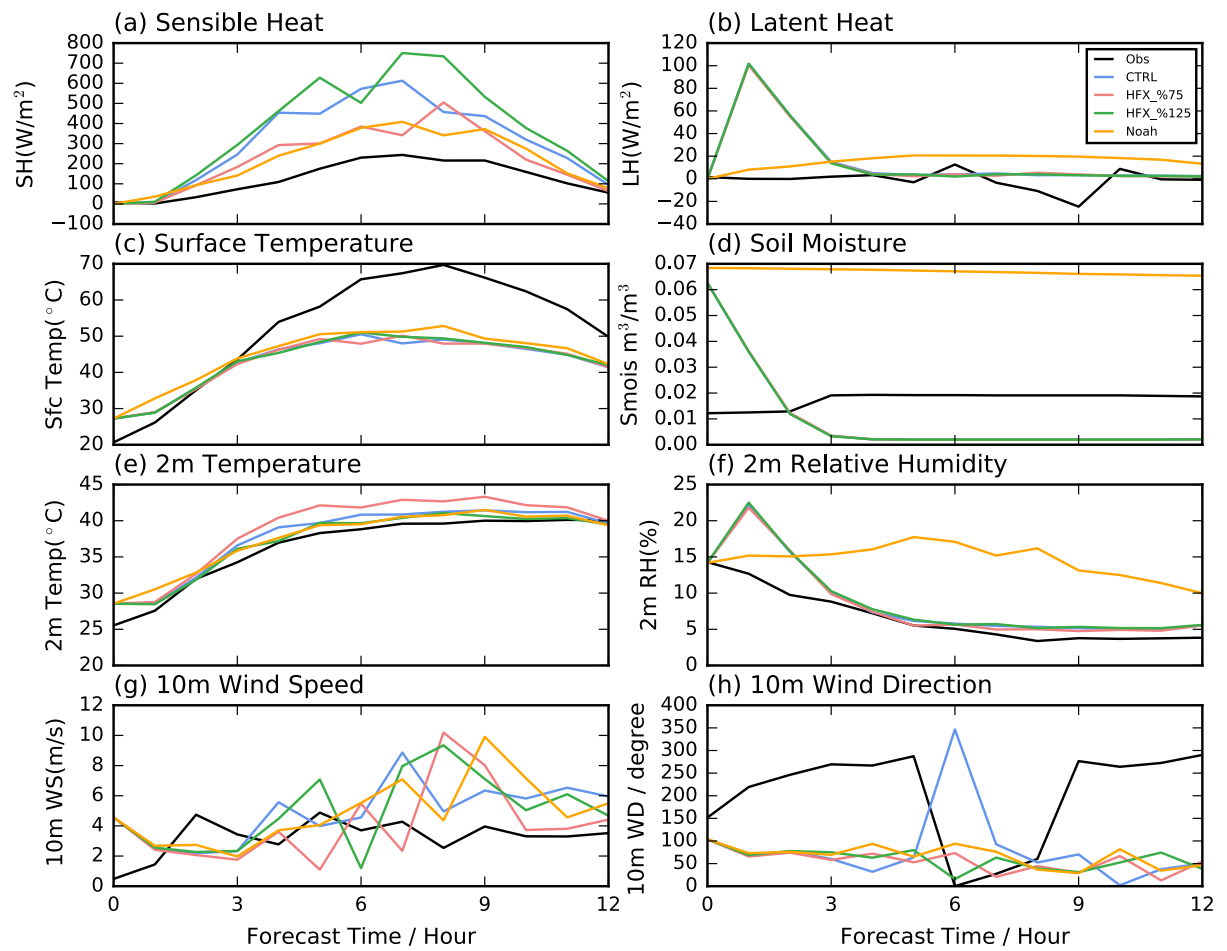


Figure 10 The same as Figure 4, but for SH flux sensitive and Noah land-surface experiment.

562

Experiment	Name	Remarks
1	BDY_T1(CTRL)	LBC of D04 is provide by d03 every 1 hour with model grids 403x406
2	BDY_T2	As BDY_T1, but LBC of D04 is provide by d03 every 6 hour
3	BDY_T3	As BDY_T2, but with model grids 205 x 208.
4	HFX_%75	As CTRL_T2, but with SH 75%.
5	HFX_%125	As CTRL_T2, but with SH 125% .
6	Noah	As CTRL_T2, but with Noah surface-land model.

563

Table 1. List of designed experiments.

564



565

Variables	Sensible Heat		Latent Heat		Surface Temperature		Soil Moisture		2m Temperature		2m Relative Humidity		10m Wind Speed	
	RMSE	BIAS	RMSE	BIAS	RMSE	BIAS	RMSE	BIAS	RMSE	BIAS	RMSE	BIAS	RMSE	BIAS
Experiments														
CTRL	263.636	250.140	12.398	6.674	14.654	-13.373	0.017	-0.017	1.666	1.613	1.220	1.109	2.579	1.864
BDY_T2	249.395	240.660	12.383	6.253	14.116	-12.853	0.017	-0.017	1.912	1.817	1.275	1.162	2.943	1.307
BDY_T3	241.681	232.705	12.251	6.328	14.929	-13.737	0.017	-0.017	1.227	1.046	1.483	1.280	2.118	1.287
HFX_%75	151.119	134.594	12.544	6.354	14.740	-13.426	0.017	-0.017	3.078	3.016	0.956	0.826	3.335	0.874
HFX_%125	357.711	335.556	12.439	6.152	14.244	-13.043	0.017	-0.017	1.026	0.860	1.303	1.231	3.265	2.052
Noah	125.695	120.313	23.350	20.664	12.757	-11.502	0.048	0.048	1.046	0.983	10.116	9.904	2.788	1.795

566

567 Table 2. Summary of surface and air variables verification including integration hours from 3 to 12 h for Tazhong station.

568

**Reference:**

- Chen, F., and J. Dudhia, 2001a: Coupling an Advanced Land Surface–Hydrology Model with the Penn State–NCAR MM5 Modeling System. Part II: Preliminary Model Validation. *Monthly Weather Review*, **129**, 587–604.
- , 2001b: Coupling an advanced land surface-hydrology model with the Penn State–NCAR MM5 modeling system. Part I: Model implementation and sensitivity. *Monthly Weather Review*, **129**, 569–585.
- Dudhia, J., 1989: Numerical study of convection observed during the winter monsoon experiment using a mesoscale two-dimensional model. *J. Atmos. Sci.*, **46**, 3077–3107.
- Engelstaedter, S., R. Washington, C. Flamant, D. J. Parker, C. J. T. Allen, and M. C. Todd, 2015: The Saharan heat low and moisture transport pathways in the central Sahara—Multi-aircraft observations and Africa-LAM evaluation. *Journal of Geophysical Research: Atmospheres*, **120**, 2015JD023123.
- Garcia-Carreras, L., and Coauthors, 2015: The Turbulent Structure and Diurnal Growth of the Saharan Atmospheric Boundary Layer. *Journal of the Atmospheric Sciences*, **72**, 693–713.
- Han, B., S. Lü, and Y. Ao, 2012: Development of the convective boundary layer capping with a thick neutral layer in Badanjinlin: Observations and simulations. *Adv. Atmos. Sci.*, **29**, 177–192.
- Heinold, B., P. Knippertz, and J. H. Marsham, 2013: Large Eddy Simulations of Nocturnal Low-Level Jets over Desert Regions and Implications for Dust Emission. *EGU General Assembly Conference*.
- Heinold, B., P. Knippertz, and R. J. Beare, 2015: Idealized large-eddy simulations of nocturnal low-level jets over subtropical desert regions and implications for dust-generating winds. *Quarterly Journal of the Royal Meteorological Society*, **141**, 1740–1752.
- Heinze, R., D. Mironov, and S. Raasch, 2015: Second-moment budgets in cloud topped boundary layers: A large-eddy simulation study. *Journal of Advances in Modeling Earth Systems*, **7**, 510–536.
- Hong, S.-Y., and H.-L. Pan, 1996: Nonlocal boundary layer vertical diffusion in a medium-range forecast model. *Monthly weather review*, **124**, 2322–2339.
- Hong, S.-Y., and J.-O. J. Lim, 2006: The WRF single-moment 6-class microphysics scheme (WSM6). *J. Korean Meteor. Soc.*, **42**, 129–151.
- Hu, X.-M., J. W. Nielsen-Gammon, and F. Zhang, 2010: Evaluation of Three Planetary Boundary Layer Schemes in the WRF Model. *Journal of Applied Meteorology and Climatology*, **49**, 1831–1844.
- Kain, J. S., 1993: Convective parameterization for mesoscale models: The Kain-Fritsch scheme. *The representation of cumulus convection in numerical models*, Meteor. Monogr, **46**, 165–170.
- Kain, J. S., 2004: The Kain–Fritsch Convective Parameterization: An Update. *JOURNAL OF APPLIED METEOROLOGY*, **43**, 170–181.
- LeMone, M. A., M. Tewari, F. Chen, and J. Dudhia, 2013: Objectively Determined Fair-Weather CBL Depths in the ARW-WRF Model and Their Comparison to CASES-97 Observations. *Monthly Weather Review*, **141**, 30–54.
- Liu, Y., Q. He, H. Zhang, and A. Mamtimin, 2012: Improving the CoLM in Taklimakan Desert hinterland with accurate key parameters and an appropriate parameterization scheme. *Adv. Atmos. Sci.*, **29**, 381–390.
- Liu, Y., and Coauthors, 2011: Simultaneous nested modeling from the synoptic scale to the LES scale for wind energy applications. *Journal of Wind Engineering and Industrial Aerodynamics*, **99**,

- 613 308-319.
- 614 Marsham, J. H., P. Knippertz, N. Dixon, D. J. Parker, and G. M. S. Lister, 2011: The importance of the  
615 representation of deep convection for modeled dust - generating winds over West Africa during  
616 summer. *Geophysical Research Letters*, **38**.
- 617 Mlawer, E. J., S. J. Taubman, P. D. Brown, M. J. Iacono, and S. A. Clough, 1997: Radiative transfer for  
618 inhomogeneous atmospheres: RRTM, a validated correlated-k model for the longwave. *J. Geophys.*  
619 *Res.*, **102**, 16663-16682.
- 620 Moeng, C.-H., J. Dudhia, J. Klemp, and P. Sullivan, 2007: Examining Two-Way Grid Nesting for Large  
621 Eddy Simulation of the PBL Using the WRF Model. *Monthly Weather Review*, **135**, 2295-2311.
- 622 National Centers for Environmental Prediction, N. W. S. N. U. S. D. o. C., 2015: NCEP GDAS/FNL  
623 0.25 Degree Global Tropospheric Analyses and Forecast Grids. Research Data Archive at the  
624 National Center for Atmospheric Research, Computational and Information Systems Laboratory.
- 625 Rai, R. K., L. K. Berg, B. Kosović, J. D. Mirocha, M. S. Pekour, and W. J. Shaw, 2017: Comparison of  
626 Measured and Numerically Simulated Turbulence Statistics in a Convective Boundary Layer Over  
627 Complex Terrain. *Boundary-Layer Meteorology*, **163**, 69-89.
- 628 Schicker, I., D. Arnold Arias, and P. Seibert, 2016: Influences of updated land-use datasets on WRF  
629 simulations for two Austrian regions. *Meteorology and Atmospheric Physics*, **128**, 279-301.
- 630 Shin, H. H., and S. Y. Hong, 2011: Intercomparison of Planetary Boundary-Layer Parametrizations  
631 in the WRF Model for a Single Day from CASES-99. *Boundary-Layer Meteorology*, **139**, 261-281.
- 632 Shin, H. H., and S.-Y. Hong, 2015: Representation of the Subgrid-Scale Turbulent Transport in  
633 Convective Boundary Layers at Gray-Zone Resolutions. *Monthly Weather Review*, **143**, 250-271.
- 634 Skamarock, W. C., and Coauthors, 2008: A Description of the Advanced Research WRF Version 3. .  
635 *NCAR/TN-475+STR, NCAR TECHNICAL NOTE*.
- 636 Smirnova Tatiana, G., M. Brown John, G. Benjamin Stanley, and D. Kim, 2000: Parameterization of  
637 cold - season processes in the MAPS land - surface scheme. *Journal of Geophysical Research:*  
638 *Atmospheres*, **105**, 4077-4086.
- 639 Smirnova, T. G., J. M. Brown, and S. G. Benjamin, 1997: Performance of Different Soil Model  
640 Configurations in Simulating Ground Surface Temperature and Surface Fluxes. *Monthly Weather*  
641 *Review*, **125**, 1870-1884.
- 642 Stull, R. B., 1988: An Introduction to Boundary Layer Meteorology. *Atmospheric Sciences Library*, **8**,  
643 89.
- 644 Sun, J., and Q. Xu, 2009: Parameterization of Sheared Convective Entrainment in the First-Order  
645 Jump Model: Evaluation Through Large-Eddy Simulation. *Boundary-Layer Meteorology*, **132**,  
646 279-288.
- 647 Talbot, C., E. Bou-Zeid, and J. Smith, 2012: Nested Mesoscale Large-Eddy Simulations with WRF:  
648 Performance in Real Test Cases. *Journal of Hydrometeorology*, **13**, 1421-1441.
- 649 ter Maat, H. W., E. J. Moors, R. W. A. Hutjes, A. A. M. Holtslag, and A. J. Dolman, 2012: Exploring the  
650 Impact of Land Cover and Topography on Rainfall Maxima in the Netherlands. *Journal of*  
651 *Hydrometeorology*, **14**, 524-542.
- 652 WANG, and Coauthors, 2016a: Summer atmospheric boundary layer structure in the hinterland of  
653 Taklimakan Desert, China. *Journal of Arid Land*, **8**, 846-860.
- 654 Wang, M., X. Xu, and H. Xu: The possible influence of the summertime deep atmospheric boundary  
655 layer process over the Taklimakan Desert on the regional weather. (*submitted to Quarterly Journal*  
656 *of the Royal Meteorological Society*).

Wang, M. Z., H. Lu, H. Ming, and J. Zhang, 2016b: Vertical structure of summer clear-sky atmospheric boundary layer over the hinterland and southern margin of Taklamakan Desert: The deep convective boundary layer of Taklamakan Desert. *Meteorological Applications*, **23**, 438-447.

Zhang, F., Z. Pu, and C. Wang, 2017: Effects of Boundary Layer Vertical Mixing on the Evolution of Hurricanes over Land. *Monthly Weather Review*, **145**, 2343-2361.

For Review Only

Dear editors and reviewers,

We deeply appreciate the time and effort you've spent in reviewing our manuscript. Your comments are really thoughtful and helpful. Thus, we revised the manuscript, following your comments exactly. We have studied comments carefully and have made correction, which we hope meet with approval. Revised portion are marked in red in the paper. The main corrections in the paper and the responds to the reviewer's comments are as flowing:

### **Reviewer: 1**

The paper is well written and presents works for PBL simulations using WRF framework. The authors explore the sensitivities of the model output due to lateral forcing of varying model sizes, frequency of the forcing, and surface heat flux. I would like the authors do some revisions on their manuscript. First, I have general comments here to address by the authors,

#### **1. I encourage the author to reorganize the Method section as 2.1 Model configuration 2.2 Data 2.3 Synoptic**

Thank you for the comments, we have reorganized the method section.

#### **2. In Model configuration, please mention how long spin-up time was used. Did authors start all domains at same time? The authors also mention 51 vertical levels but you did not give what resolutions they are, particularly within the boundary layer. Please mention this.**

Yes, we start all domains at same time. Height for lowest 20 levels are 1130.473, 1157.705, 1207.765, 1294.703, 1423.873, 1591.895, 1795.526, 2021.868, 2272.33, 2558.433, 2882.675, 3248.113, 3658.499, 4118.481, 4633.882, 5212.111, 5855.802, 6517.111, 7151.295, 7757.151.

#### **3. The authors have presented several figures (vertical profiles and time series) but they have not mentioned how the plots are generated. Give details what the plots are representing – instantaneous or time/space averaged.**

Thank you for the comments, we have added more details about profiles and series as follow:

Figure 4 Vertical profiles of potential temperature (solid line, units: K) and vapor mixing ratio(dash line, units: g/Kg)**from innermost domain of simulations and observation of GPS sounding at Tazhong station (83.63° E, 39.03° N)** at (a)1100 (b) 1400 (c) 1700 (d) 2000 BJT 01 Jul2016.

Figure 5 Time series of simulated surface **variables from innermost domain of simulations and surface observations at Tazhong station (83.63° E, 39.03° N)** initial at 0800 BJT 01July 2016 (a) sensible heat flux (W/m<sup>2</sup>), (b) latent heat flux(W/m<sup>2</sup>), (c) 2-m temperature (°C), (d) surface temperature (°C), (e) 2-m Relative Humidity(%) and (f) 10-m wind speed (m/s ) with corresponding observations.

4. I guess the results from the innermost domain d04 are obtained without using perturbation near the inflow boundaries. It is not unexpected to see the difference in model output due to the varying grid size when the grid size reduces by more than half area. Similarly, more frequent forcing (1 hr) also provide more turbulence into the nested domain compared to 6 hr, as the model linearly interpolates tendencies between 6 hours. In this regard, it is always good to check how long fetch it took to develop the turbulence. Is the turbulence developed at the location where the model output is tapped? Have you checked results for other locations, may be far from the inflow boundaries where turbulence is well developed?

We have added instantaneous vertical velocity fields for the horizontal (Figure 7) and vertical cross-sections along Tazhong station (39°N) of vertical velocity(Figure 8).

The instantaneous vertical velocity fields for the horizontal are displayed in Figure 7. By 1400 BJT, the convection of CTRL simulation obviously intensified under strong surface heating (Xu et al. 2018). Thus, the maximum vertical velocity reaches 9 m/s and the depth of mixed layer grows to about 4.3 km (Figure 7 a). The distances between the boundary layer rolls correspondingly increase to about 12 km and the height of the peak updraughts is raised to just under 4 km. The cellular

shape of updraughts and downdraughts characteristic of boundary layer rolls is obvious in the horizontal view with the strength of convection. BDY\_T2 and BDY\_T3 experiments (Figure 7 b, c). both reproduce motions with much weaker maximum and minimum values at boundary of domain. In BDY\_T3 experiment, Tazhong station at center of the model has been directly influenced by the inflow cold advection produced by low frequency LBCS and results in much weaker maximum and minimum value of  $w$  (about 6 m/s). However, despite the underestimate of potential temperature, the  $w$  fields for BDY\_T2 experiment look similar to the CTRL  $w$  in plain view, and the horizontal extent of the updrafts/downdrafts agrees with the CTRL as can be inferred from Figure 7. To further examine the impact of LBCS on the simulation of desert CBL vertical cross-sections along Tazhong station ( $39^{\circ}\text{N}$ ) of vertical velocity are presented in Figure 8. Wide and regularly spaced updrafts along A1- A2 split into the stronger and more irregular motions in CTRL and BDY\_T2. The updrafts are much weaker in the BDY\_T3 experiment, as can be seen from Figure 8 c. Peak updrafts on BDY\_T3 are about 4 m/s much weaker than on CTRL (9 m/s) and BDY\_T2 (8 m/s). For BDY\_T2 and BDY\_T3, the distant of the inflow boundary is wider, and the intensity of the convection is weaker at the boundary. Compared with BDY\_T2, the horizontal distribution of vertical velocity at Tazhong station in BDY\_T3 experiments is much weaker.

**5. I encouraged to run an additional simulation with different land-surface model as the authors mentioned that the heat flux and moisture quantities are playing the PBL growth.**

Thank you for the comments, we have run an additional simulation with Noah land-surface model.

**6. The authors tested with varying sensible heats in the simulation. I could not see the results of that in the manuscript. Could you present them together in figures 4-6 so that it helps reader to compare with other results?**

Thank you for the comments and sorry for the mistake, Figure 8 and Figure 9 are the results from simulations with varying sensible heats. We have redrawn potential temperature and vapor mixing ratio into one figure. The new figure

also contains the results from Noah land-surface model as mentioned in comment 5.

**7. In Fig. 7, I could not follow why the sizes of vertical cross-section is different between the panels in the first and the rest**

Thank you for the comments and sorry for the mistake, we have reordered the Fig. 7(Figure 6 in the present manuscript), and modified BDY\_T1 to BDY\_T3. The sizes of vertical cross-section are different between the panels in BDY\_T3 and the rest, because Sizes of BDY\_T3 (205 X 208) is much smaller than the others(403X406).

**8. I found cumbersome to go back and forth for the figures as the order of figures are random. Please put the figure in order. Similarly, the authors presented figures 8 and 9 in the list of figures, but I could not come across with those figures in the manuscript. Am I missing somewhere?**

Thank you for the comments. We have reordered the figures. Figure 8 and Figure 9 are the results from simulations with varying sensible heats. Furthermore, we have put potential temperature and vapor mixing ratio into Figure 7.

**9. When reading introduction, it looks like this work (desert case) is the first of its kind. Please make sure this. In addition, the authors may also mention complex terrain real case by Rai et al. (2017), where they did evaluate the turbulence statistics for the convective PBL in terms of turbulence model, domain size etc.**

Thank you for the comments. We have cited the study, and changed the introduction.

Specific comments

1. Line 68: provide reference for '... 4-6 km during ...'.

Ok

2. Line 67 and 69: use either ABL or PBL and define it for the first time

Thank you for the comments. We have changed all ABL to PBL.

3. Line 129: why the section starts with 1, but not for introduction?

Thank you for the comments. We have changed introduction to the first section.

4. Line 144: define BJT



Thank you for the comments. We have changed BJT to BJT (Beijing Time)

5. Line 149-150: move to section model configuration

Ok

6. Line 164: make clear what is two experiments?

Thank you for the comments. We have changed 'Figure 1 shows the domain for two experiments.' to 'Figure 1 shows the domain for all experiments except for BDY\_T3. Smaller grid sizes (205 x 208) are used in experiment BDY\_T3 to verify the effect of domain size on LES simulation.'

7. Line 173: use space in '... millibars(National ....'. Check this throughout the manuscript as I found they occurs everywhere.

Ok

8. Line 185-186: check sentence syntax for 'For one-way nest, ...'

Thank you for the comments. We have changed 'For one-way nest, Specified LBC obtained from coarser model simulation.' to 'For one-way nest, specified LBC is obtained from coarser model simulation.'

9. Line 218: define SH

We have change 'SH' to 'SH (surface sensible heat flux)'.

10. Line 245: see the period

Ok.

11. Line 279: it to It?

Ok.

12. Line 341-342: check the sentence syntax

Ok.

13. Line 351: the to The?

Ok.

Reviewer: 2

General comments

Characteristics of the convective boundary layer (CBL) over desert(s) are not

well defined due to lacking of observational data and high resolution numerical simulations. It definitely represents one of the research interests for the atmospheric boundary layer meteorology, weather, and climate. In this manuscript, the authors attempted to present the performance of WRF/LES on simulating the CBL structures and their evolution over the Taklimakan Desert during the summer daytime. They presented how the simulated vertical profiles of potential temperature and specific humidity were sensitive to the ingest frequency of lateral boundary conditions, and how the on simulated vertical profiles changed with surface heat fluxes. It is not surprised that the WRF/LES simulations with hourly update of lateral boundary conditions ingest showed better agreement with the observations (see Figure 4.b). The findings obtained from these two group sensitivity studies are not new at all. As indicated by the manuscript title, the study is supposed to focus on the performance of WRF/Chem. No enough meaningful evaluation results are provided in the manuscript to support the objective indicated by the manuscript title. The manuscript structure isn't well designed. Scientific questions are not clearly defined and insightful analyses are lacking. Extensive grammar errors make the manuscript very difficult to read and understand. No significant results were obtained from this study. Therefore, the manuscript is suggested to reject given the current status.

Major comments

**1. Observation-simulation comparisons (e.g., time series and vertical profiles) and statistical evaluations of the model simulation (considered as a base case) should be presented before the sensitivity studies (sections 3.1 and 3.2).**

Thank you for the comment. We have reordered the section 3.1 and section 3.2.

**2. How are the lateral boundary conditions of the innermost domain**

**updated during the simulations? Is it not updated every integration time step? It is not useful to present sensitivity studies on impact of updated frequency of lateral boundary layer conditions on the WRF/LES results.**

Thank you for the comments. We conducted one-way nest WRF from mesoscale down to LES-scales. For one-way nest, Specified LBC is obtained from coarser model simulation. For innermost, all forecast times from d03 simulation are used to specify the LBC. Limited by storage of our supercomputer, all model results are in 1hour interval.

As in Talbot et al. (2012), LES model fields are primarily influenced by their mesoscale meteorological forcing. Thus, in this study, we want to further examine the impact of uncertainties of LBC on LES simulation. The results suggest that the model results are sensitive to changes in time resolution and domain size of Specified LBC. The mismatch among sensitive experiments is present means that the effect of LBC needs to be quantified to realize a more realistic performance in the sub-kilometer simulations.

**3. Why the vertical profiles of specific humidity (Figure 5) are very different from those of potential temperature (Figure 4) within the CBL. Is this the real case? What are the main reasons causing such type of vertical distribution?**

Yes, it's the real case. We also find inverse humidity in July 2017. Inverse humidity may be caused by the joint of the heterogeneous humidity Pattern and Large-scale advection over the underlying surface. For instance, interaction of oasis with desert environment may resulted in the inverse humidity layer in desert PBL.

**4. Why is the maximum observed surface sensible heat flux less than 250 W·m<sup>-2</sup>? This is not consistent with the boundary layer height (up to 5000 m). Is it possible to observe such low sensible heat flux over the desert?**

Thank you for the comments,

(1) it should be noted that the SH and LH based on eddy correlation might be underestimated. Researchers found that if the other two terms in the budget—net radiation and flux into the soil were accurate, used data for the whole experiment to find the  $H + LE$  are equal to an average of 75% of what would be required for balancing the surface energy budget (LeMone et al. 2013). Under this scenario, the government would soon recoup its investment and the debt pile would shrink.

(2) RL (residual layer) may play a key role in the deep PBL at Taklimakan desert. At 1100 BJT, when the PBLH was about 300 m in observation as shown above, potential temperature in the PBL was about 317 K and 320 K in RL, respectively. When the potential temperature in CBL increased to 320 K because of heating from under layer surface, the CBL merged with the RL, and the height of PBL reached 3000 m in the observations at 1400 BJT. These results are in good agreement with Han et al. (2012). By analysis of observation of a CBL in the Badanjilin region, they found a rapid development process of CBL after 1200 LST, which appeared to be a jump of PBLH when the inversion layer vanished.

(3) Results of simulations on desert PBL in the morning agree with the previous studies of sensitivities land-surface model for other areas (Hu et al. 2010; Zhang et al. 2017). However, during 1700~2000 BJT 01 July (Figure 9b, d), all experiments produce nearly the same CBLH and moisture in agreement with observation in the PBL. The effects of SH on the evolution of Taklimakan PBL structures during this period are needed to be further examined and discussed. So, the question is: why are simulations insensitive to land-surface process by the end of the day? As in Stull (1988), the development of CBL is mainly influenced by the effect of thermodynamic and turbulent entrainment without considering large scale factors such as large scale advection or subsidence. Besides the surface sensible heat, the intensity of entrainment process determines the increasing rate of CBL. Thus, the entrainment rate  $w_e$  is a valuable indicator for the development of PBL structure.

The rate of growth of the convective boundary layer is mainly determined by the entrainment rate  $w_e$  at the inversion layer without considering large scale

vertical motion.  $w_e$  usually has a positive correlation with heat flux amount at the inversion layer  $\overline{(w'\theta_v')_h}$ , and large LES experiments show  $\overline{(w'\theta_v')_h}$  is about 0.2 times the surface flux of buoyancy  $\overline{(w'\theta_0')}$ . During the period from 1100 to 1400 BJT, larger  $SH$  is obviously correlated with stronger turbulent entrainment and warmer air from free atmosphere (FA) entraining into ML. As a result, CBL develop rapidly and is warm too fast in the early simulation phase due to the obviously increasing temperature and strong vertical mixing in model. Of interesting is that reduction in  $SH$  reproduces better desert PBL evolution in the early simulation phase, as  $SH-75\%$  and Noah produce the smallest simulation errors in both temperature and moisture. However, one should note that CBLH and potential temperature for  $SH-75\%$  and Noah have reached above 5000 m and 323.2 K respectively at 1700 BJT (Figure 9a). For the rest of the day, the increase rate of CBL height slows down due to the deep CBL(>5000m) which require more heat for the growth of PBL depth; Moreover,  $w_e$  decrease with increasing inversion intensity, which inhibits the mixing and entrainment processes. These two factors obviously limit the growth of CBL when CBLH is over 5000 m in this deep desert CBL case. Therefore, increasing  $SH$  from 75% to 125% significantly reduce the total time needed for CBL increase to a relative low altitude (< 5 km) at the middle and preliminary stage of the development of CBL rather than produce higher CBL at the late stage. When height of CBL over Taklimakan desert exceeds 5000 m, it might not change with proportion to  $SH$  fluxes (Figure 9d). As a result, PBL of WRF simulations are basically the same, and not sensitive to  $SH$  fluxes by the end of the day.

**5. It is required to calculate statistical parameters for the model evaluation.**

Thank you for your comments, we have added 'Summary of surface and air variables verification including integration hours from 3 to 12 h for Tazhong station.' in Table 2.

**6. L206-207: How the more frequently LBCs may cause the cold advection?**

Sorry for the mistake, we have changed 'The more frequently updated LBC is

desirable to cold zone near the LBC, which results in cold advection of the temperature and moisture to the area of interest' to 'The lower frequently updated LBC is desirable to cold zone near the LBC, which results in cold advection of the temperature and moisture to the area of interest'.

Lower frequently LBCs may cause the cold advection, because earlier model results from d03 simulation are used to specify the LBC, which. In this case, BDY\_T2 and BDY\_T3 experiment LBC with 6 interval results from D03 produced cold zone in the lateral boundaries, and resulted in the cold advection.

**7. The authors pointed out that the soil moisture was over-estimated by the model and initial soil moisture is higher than the observations (see L242-243, L248-250). If this is the case, the sensible could be under-predicted. However, the simulation results show the over-prediction of sensible heat flux by the model (see L218-220).**

Thank you for the comments. Yes, the large overestimate of soil moisture makes LH (Figure4 b, f) from the model continue to increase. As a result, near-surface of model is far moister than that of observation at the first few hours of model integration. However, an interesting result to be note is that the model simulation has the abilities to correct some of the bias due to the initial condition of the surface; The results from CTRL experiment are closer to observation after 3 hours' spin-up. Thus, the large overestimate of soil moisture at initial stage(0~3hours) may have little impact on the large over-prediction of sensible heat flux during 3~9 hours' simulation.

**8. As pointed out by the authors that the surface heat flux is the main driving force to the boundary layer growth. The model captured the boundary layer height quite well (see the control case in Figure 4.d) even the surface heat flux is significantly over-predicted by the model (see Figure 6).**

Results of simulations on desert PBL in the morning agree with the previous studies of sensitivities land-surface model for other areas (Hu et al. 2010; Zhang et al. 2017). However, during 1700~2000 BJT 01July (Figure 9b, d), all experiments produce nearly the same CBLH and moisture in agreement with observation in the

PBL. The effects of SH on the evolution of Taklimakan PBL structures during this period are needed to be further examined and discussed. So, the question is: why are simulations insensitive to land-surface process by the end of the day? As in Stull (1988), the development of CBL is mainly influenced by the effect of thermodynamic and turbulent entrainment without considering large scale factors such as large scale advection or subsidence. Besides the surface sensible heat, the intensity of entrainment process determines the increasing rate of CBL. Thus, the entrainment rate  $w_e$  is a valuable indicator for the development of PBL structure.

The rate of growth of the convective boundary layer is mainly determined by the entrainment rate  $w_e$  at the inversion layer without considering large scale vertical motion.  $w_e$  usually has a positive correlation with heat flux amount at the inversion layer  $\overline{(w'\theta_v')_h}$ , and large LES experiments show  $\overline{(w'\theta_v')_h}$  is about 0.2 times the surface flux of buoyancy  $\overline{(w'\theta_0')}$ . During the period from 1100 to 1400 BJT, larger SH is obviously correlated with stronger turbulent entrainment and warmer air from free atmosphere (FA) entraining into ML. As a result, CBL develop rapidly and is warm too fast in the early simulation phase due to the obviously increasing temperature and strong vertical mixing in model. Of interesting is that reduction in SH reproduces better desert PBL evolution in the early simulation phase, as SH-75% and Noah produce the smallest simulation errors in both temperature and moisture. However, one should note that CBLH and potential temperature for SH-75% and Noah have reached above 5000 m and 323.2 K respectively at 1700 BJT (Figure 9a). For the rest of the day, the increase rate of CBL height slows down due to the deep CBL(>5000m) which require more heat for the growth of PBL depth; Moreover,  $w_e$  decrease with increasing inversion intensity, which inhibits the mixing and entrainment processes. These two factors obviously limit the growth of CBL when CBLH is over 5000 m in this deep desert CBL case. Therefore, increasing SH from 75% to 125% significantly reduce the total time needed for CBL increase to a relative low altitude (< 5 km) at the middle and preliminary stage of the development of CBL rather than produce higher CBL at the late stage. When height of CBL over

Taklimakan desert exceeds 5000 m, it might not change with proportion to SH fluxes (Figure 9d). As a result, PBL of WRF simulations are basically the same, and not sensitive to SH fluxes by the end of the day.

**9. Entrainment process could play an important role in the CBL development over the Desert. However, it hasn't discussed by the authors.**

As in comment 8.

**10. There are too many grammar errors throughout the manuscript. It is difficult to list all the errors here.**

We have carefully revised the manuscript according to the reviewers' comments, and also have rescrutinized to improve the English by a native English speaker.

**Reviewer: 3**

### **Major comments**

#### **1 Observation**

**The observation site is located in the center of desert. As the author says, the PBL there can reach 5000 m. Is this conclusion just based on the observation results given in fig.4 and 5? Or this results has been mentioned in other study from more atmospheric profiles? In my opinion, profiles only in one day cannot represent the common structures of low atmosphere as well as PBL. To state that the PBL in this desert can reach 5000 m frequently instead of occasionally, more profiles need to be given. Maybe the author can found some other similar research to support their conclusion.**

The conclusion of desert PBL can reach 5000 m is based on the study of Wang et.al. They statics the PBL height of Tazhong and four surrounding stations (Minfeng, Korla, Ruoqiang and Kashgar, Figure b1) during July 2016. The number of days when



the ABL exceeds 4,000 m depth is 8, 9, 5, 4 and 2 respectively, and that of higher than 3,000 m is 20, 22, 13, 15, and 5 respectively.

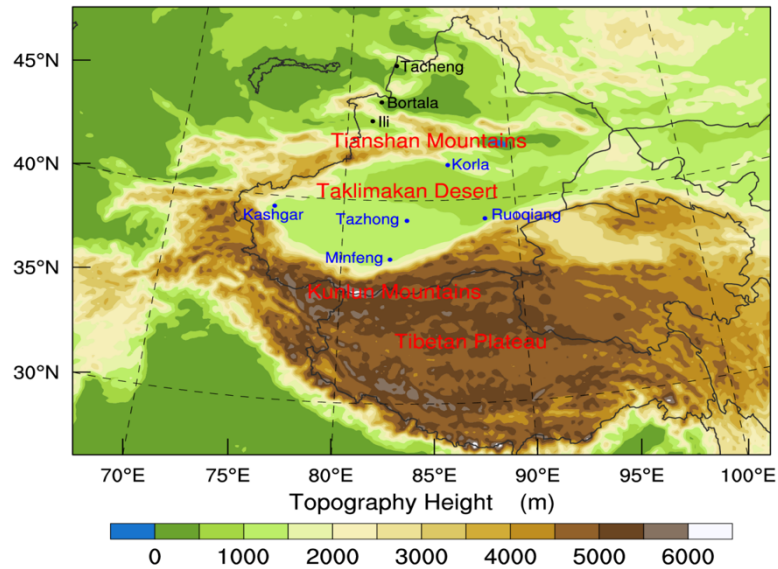


**Figure b1.** Location of the sounding stations.

**Table 3.** The number of days with deep boundary layers in the hinterland and the surrounding areas of the Taklimakan Desert in July 2016.

Height of the boundary layer	Tazhong	Minfeng	Korla	Ruoqiang	Karshgar
$\geq 5000$ m	1	1	1	1	0
$\geq 4000$ m	8	9	5	4	2
$\geq 3500$ m	15	17	6	9	4
$\geq 3000$ m	20	22	13	15	5

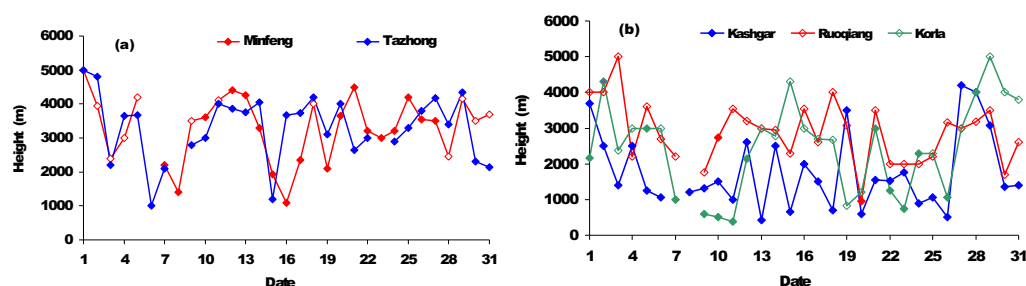


**Figure b2.** Curves of the daily height variations of the boundary layers in the hinterland and the surrounding areas of the Taklimakan Desert at 19:15 in July 2016.

(The solid symbols representing the height of the convective boundary layer while the hollow symbols representing the height of the residual mixed layer)

## 2 WRF-LES

**The author compare the results from WRF-LES to that from radio sounder. It should be noted that the radiosounder also floated horizontally during its raising. The distance of horizontal displacement, generally 1-30 km if the radiosounder can reach 20 km high, depend on the horizontal wind. The horizontal movement can be ignored if the grid size of numerical model is larger than 20 km, but as for this study, the grid size is 330m, the effect of horizontal movement should be state in this study.**

Yes, when radio-sounder reach 6km height, it floating about 7Km away. Thus, for more accuracy, we have averaged the profile of model output center at Tazhong station in 3.5km radius.

**The author should also state why choosing WRF-LES, instead of LES or one-dimension PBL model, in study.**

Thank you for the comment.

(1) As in Xu et al. (2018), we have examined impact of PBL schemes on simulating deep PBL over Taklimakan dessert. Results show that there are still uncertainties, despite of using the state-of-the-art scale dependencies PBL scheme with reference data from LES.

(2) The aim of this paper is to examine assess the skillfulness of WRF-LES in relative coarse resolution (333m) over Taklimakan dessert, in simulating real cases of desert PBL process during boreal summer events in Taklimakan.

WRF-LES can give the 3-D structure of lower atmosphere, but I note only fig.7 shows such results, and the corresponding statement in the manuscript seems contributed little to the main conclusion. I suggested that the authors add some discussion on the horizontal distribution of PBL or lapse rate of lower atmosphere over the desert region, and given a detailed description on the effect of advection in the night before the day of radio sound launched. By doing this, the difference in initial profile between observation and simulation may be better understand.

Thank you for the comment. We have added instantaneous vertical velocity fields for the horizontal (Figure 7) and vertical cross-sections along Tazhong station ( $39^{\circ}$  N) of vertical velocity (Figure 8).

The instantaneous vertical velocity fields for the horizontal are displayed in Figure 7. By 1400 BJT, the convection of WRF-LES simulation obviously intensified under strong surface heating (Xu et al. 2018). Thus, the maximum vertical velocity reaches 9 m/s and the depth of mixed layer grows to about 4.3 km (Figure 7 a). The distances between the boundary layer rolls correspondingly increase to about 12 km and the height of the peak updrafts is raised to just under 4 km. The cellular shape of updrafts and downdrafts characteristic of boundary layer rolls is obvious in the horizontal view with the strength of convection. BDY\_T2 and BDY\_T3 experiments (Figure 7 b, c), both reproduce motions with much weaker maximum and minimum values at boundary of domain. In BDY\_T3 experiment, Tazhong station at center of the model has been directly influenced by the inflow cold advection produced by low frequency LBCS and results in much weaker maximum and minimum value of (about 6 m/s). However, despite the underestimate of potential temperature, the fields for BDY\_T2 experiment look similar to the CTRL in plain view, and the horizontal extent of the updrafts/downdrafts agrees with the CTRL as can be inferred from Figure 7. To further examine the impact of LBCS on the simulation of desert CBL vertical cross-sections along Tazhong station ( $39^{\circ}$  N) of vertical velocity are presented in Figure 8. Wide and regularly spaced updrafts along A1-A2 split into the stronger and more irregular motions in CTRL and BDY\_T2. The updrafts are much weaker in the BDY\_T3 experiment, as can be seen from Figure 8 c. Peak updrafts on BDY\_T3 are about 4 m/s much weaker than on CTRL (9 m/s) and BDY\_T2 (8 m/s). For BDY\_T2 and BDY\_T3, the distant of the inflow boundary is wider, and the intensity of the convection is weaker at the boundary. Compared with BDY\_T2, the horizontal distribution of vertical velocity at Tazhong station in BDY\_T3 experiments is much weaker.

### 3 Land surface model

The difference in surface flux between simulation and observation seems to be too large, especially for the sensible heat flux (SH). The peak SH is about  $250 \text{ Wm}^{-2}$ , but all simulations give the peak SH to be  $\sim 600 \text{ Wm}^{-2}$ . As the author mentioned, SH is a key factor to the development of convective boundary layer. If the land surface model give a similar SH as observed, is the 5000 m high PBL can still be given in all simulation cases? If not/so, why? Did the author verified all crucial parameterization schemes (like PBL, LSM etc.) before all simulations start? I also noted the simulated latent heat flux is also greater than the observed one, which infers the net radiation at land surface might be overestimated too. The author mentioned the USGS land use data might be problematic, but no detailed information has been given. For example, is the albedo between observation and simulation comparable? Only if the surface parameters and process are properly given, the PBL process, which is a combination of land surface process and free atmosphere dynamic processes, in numerical model can be more sound and meaningful.

**If the land surface model give a similar SH as observed, is the 5000 m high PBL can still be given in all simulation cases? If not/so, why?**

Results of simulations on desert PBL in the morning agree with the previous studies of sensitivities land-surface model for other areas (Hu et al. 2010; Zhang et al. 2017). However, during 1700~2000 BJT 01July (Figure 9b, d), all experiments produce nearly the same CBLH and moisture in agreement with observation in the PBL. The effects of SH on the evolution of Taklimakan PBL structures during this period are needed to be further examined and discussed. So, the question is: why are simulations insensitive to land-surface process by the end of the day? As in Stull (1988), the development of CBL is mainly influenced by the effect of thermodynamic and turbulent entrainment without considering large scale factors such as large scale advection or subsidence. Besides the surface sensible heat, the intensity of entrainment process determines the increasing rate of CBL. Thus, the entrainment rate  $w_e$  is a valuable indicator for the development of PBL structure.

The rate of growth of the convective boundary layer is mainly determined by the entrainment rate  $w_e$  at the inversion layer without considering large scale vertical motion.  $w_e$  usually has a positive correlation with heat flux amount at the inversion layer  $\overline{(w'\theta_v')_h}$ , and large LES experiments show  $\overline{(w'\theta_v')_h}$  is about 0.2 times the

surface flux of buoyancy  $\overline{(w'\theta_0')}$ . During the period from 1100 to 1400 BJT, larger  $SH$  is obviously correlated with stronger turbulent entrainment and warmer air from free atmosphere (FA) entraining into ML. As a result, CBL develop rapidly and is warm too fast in the early simulation phase due to the obviously increasing temperature and strong vertical mixing in model. Of interesting is that reduction in  $SH$  reproduces better desert PBL evolution in the early simulation phase, as SH-75% and Noah produce the smallest simulation errors in both temperature and moisture. However, one should note that CBLH and potential temperature for SH-75% and Noah have reached above 5000 m and 323.2 K respectively at 1700 BJT (Figure 9a). For the rest of the day, the increase rate of CBL height slows down due to the deep CBL(>5000m) which require more heat for the growth of PBL depth; Moreover,  $w_e$  decrease with increasing inversion intensity, which inhibits the mixing and entrainment processes. These two factors obviously limit the growth of CBL when CBLH is over 5000 m in this deep desert CBL case. Therefore, increasing  $SH$  from 75% to 125% significantly reduce the total time needed for CBL increase to a relative low altitude (< 5 km) at the middle and preliminary stage of the development of CBL rather than produce higher CBL at the late stage. When height of CBL over Taklimakan desert exceeds 5000 m, it might not change with proportion to  $SH$  fluxes (Figure 9d). As a result, PBL of WRF simulations are basically the same, and not sensitive to  $SH$  fluxes by the end of the day.

**Did the author verified all crucial parameterization schemes (like PBL, LSM etc.) before all simulations start? I also noted the simulated latent heat flux is also greater than the observed one, which infers the net radiation at land surface might be overestimated too. The author mentioned the USGS land use data might be problematic, but no detailed information has been given. For example, is the albedo between observation and simulation comparable? Only if the surface parameters and process are properly given, the PBL process, which is a combination of land surface process and free atmosphere dynamic processes, in numerical model can be more sound and meaningful.**

(1) Yes, we have verified PBL parameterization schemes. As in Xu et al. (2018), we have verified impact of different PBL schemes on the same case as this study.

(2) We also added an experiment with Noah LSM to be compare to the RUC LSM used in CTRL experiment.

(3) To verify the influence of landuse on overestimate of SH, the albedo of observation is calculated from upward show wave radiation and downward. Results show that albedo from observation (0.239) is in agreement with that of CTRL (0.21) experiment. This indicates that difference of landuse between model and observation are not the key reason for overestimate of SH.

(4) However, One possible reason for inverse humidity may be caused by the error in landuse. Inverse humidity may be caused by the joint of the heterogeneous humidity Pattern and Large-scale advection over the underlying surface. For instance, interaction of oasis with desert environment may resulted in the inverse humidity layer in desert PBL.

#### 4 Conclusions

**One of the main conclusion is that the surface sensible flux is essential to the simulation of PBL, which is a common realization of PBL development because the buoyancy flux is main forcing of convective boundary layer rather than wind shear. However, from the sensitive experiment, when SH changed significantly, the shape of atmospheric profile did not show similar magnitude of change, and I guess the height of PBL did not increase/decrease for 25% (the author mentioned the change of PBL height should be 15% in Abstract, but I cannot found similar statement in section 3.3). How the height of PBL were defined should also be given in the manuscript. I noted that the residual layer at 1100 BJT is neutral and deep, is it the main reason for the deep PBL instead of SH? The author can refer to the work of Han in AAS in 2012.**

Yes, RL(residual layer) may play a key role in the deep PBL.

(1) One should note that RL (residual layer) play a key role in the deep PBL at Taklimakan desert. At 1100 BJT, when the PBLH was about 300 m in observation as show above, potential temperature in the were about 317 in PBL and 320 K in RL, respectively. When the potential temperature in CBL increased to 320 K because of

heating from under layer surface, the CBL merged with the RL, and the height of PBL reach 3000m in the observations at 1400 BJT. These results are in good agreement with Han et al. (2012). By analysis of observation of a CBL in the Badanjilin region, they found a rapid development process of CBL after 1200 LST, which appeared to be a jump of PBLH when the inversion layer vanished.

(2) As in comment 4. The rate of growth of the convective boundary layer is mainly determined by the entrainment rate  $w_e$  at the inversion layer without considering large scale vertical motion.  $w_e$  usually has a positive correlation with heat flux amount at the inversion layer  $\overline{(w'\theta_v')_h}$ , and large LES experiments show  $\overline{(w'\theta_v')_h}$  is about 0.2 times the surface flux of buoyancy  $\overline{(w'\theta_0')}$ . During the period from 1100 to 1400 BJT, larger  $SH$  is obviously correlated with stronger turbulent entrainment and warmer air from free atmosphere (FA) entraining into ML. As a result, CBL develop rapidly and is warm too fast in the early simulation phase due to the obviously increasing temperature and strong vertical mixing in model. Of interesting is that reduction in  $SH$  reproduces better desert PBL evolution in the early simulation phase, as  $SH-75\%$  and Noah produce the smallest simulation errors in both temperature and moisture. However, one should note that CBLH and potential temperature for  $SH-75\%$  and Noah have reached above 5000 m and 323.2 K respectively at 1700 BJT (Figure 9a). For the rest of the day, the increase rate of CBL height slows down due to the deep CBL(>5000m) which require more heat for the growth of PBL depth; Moreover,  $w_e$  decrease with increasing inversion intensity, which inhibits the mixing and entrainment processes. These two factors obviously limit the growth of CBL when CBLH is over 5000 m in this deep desert CBL case. Therefore, increasing  $SH$  from 75% to 125% significantly reduce the total time needed for CBL increase to a relative low altitude (< 5 km) at the middle and preliminary stage of the development of CBL rather than produce higher CBL at the late stage. When height of CBL over Taklimakan desert exceeds 5000 m, it might not change with proportion to  $SH$  fluxes (Figure 9d). As a result, PBL of WRF

simulations are basically the same, and not sensitive to SH fluxes by the end of the day.

#### Minor comments

Some statements may confuse the readers, I listed them below.

1 P4L91" ... mesoscale atmospheric models are still cannot...",-> unable to?

Ok, we have changed 'still cannot' to 'still unable to'.

2 P6L136 "The high-pressure system at low level, which is termed of heat low (Figure 3)," is this system high pressure or not?

We have changed "The high-pressure system at low level, which is termed of heat low (Figure 3)," to "The low-pressure system at low level, which is termed of heat low (Figure 3),"

#### Editor(s)' Comments to Author:

Editor: 1

Comments to the Author:

I have thought long-and-hard about this work since the reviews were so disparate (one reviewer suggested rejection). So I urge you to strongly consider carefully addressing the comments, particularly better examining the importance of land-surface processes and entrainment, as well as improving writing.

Ok

The 1st reviewer encouraged more sensitivity simulations and investigation, particularly in terms of importance of land-surface processes and inflow fetch. Also the reviewer raised a lot of issue in terms of writing! Please be very careful and make sure present your results nicely!

Ok

The 2nd reviewer is most critical. He suggested more examination of role of land surface fluxes and entrainment process on the development of CBL. Actually the 3rd reviewer suggested the same issue (e.g., importance of residual layer is nearly equivalent as the importance of entrainment in terms of CBL development). BTW, a lot of existing papers discussed the entrainment, which should be cited.

Also the 2nd reviewer pointed out the writing of the manuscript needs significant improvement, including organization, introduction, and grammar.

Ok

The 3rd reviewer suggested more discussion, particularly importance of land surface processes/fluxes on the development of PBL, as well as the role of pre-existing residual layer, and impact of horizontal drifting of the sounds.



Ok

**Please put profiles of potential temperature and water vapor mixing ratio side by side since they can collectively indicate the boundary layer structure, that is, combine Figures 4 & 5; Figures 8&9**

Thank you for your comments, We have redraw Figures 4 & 5 and Figures 8&9 into Figure 5 and Figure 7 respectively.

## Reference

- Hu, X.-M., J. W. Nielsen-Gammon, and F. Zhang, 2010: Evaluation of Three Planetary Boundary Layer Schemes in the WRF Model. *Journal of Applied Meteorology and Climatology*, **49**, 1831-1844.
- LeMone, M. A., M. Tewari, F. Chen, and J. Dudhia, 2013: Objectively Determined Fair-Weather CBL Depths in the ARW-WRF Model and Their Comparison to CASES-97 Observations. *Monthly Weather Review*, **141**, 30-54.
- Stull, R. B., 1988: An Introduction to Boundary Layer Meteorology. *Atmospheric Sciences Library*, **8**, 89.
- Talbot, C., E. Bou-Zeid, and J. Smith, 2012: Nested Mesoscale Large-Eddy Simulations with WRF: Performance in Real Test Cases. *Journal of Hydrometeorology*, **13**, 1421-1441.
- Wang, M., X. Xu, and H. Xu: The possible influence of the summertime deep atmospheric boundary layer process over the Taklimakan Desert on the regional weather. (*submitted to Quarterly Journal of the Royal Meteorological Society*).
- Xu, H., Y. Wang, and M. Wang, 2018: The Performance of a Scale-Aware Nonlocal PBL Scheme for the Subkilometer Simulation of a Deep CBL over the Taklimakan Desert. *Advances in Meteorology*, **2018**, 12.
- Zhang, F., Z. Pu, and C. Wang, 2017: Effects of Boundary Layer Vertical Mixing on the Evolution of Hurricanes over Land. *Monthly Weather Review*, **145**, 2343-2361.

1       **Performance of WRF Large-Eddy Simulations in summertime CBL**  
2       **characteristics over the Taklimakan Desert: A Real Test Case**

3  
4  
5               Hongxiong Xu<sup>1</sup>, Minzhong Wang<sup>124</sup>, Yinjun Wang<sup>1</sup>, Wenyue Cai<sup>13</sup>  
6

7  
8  
9  
10  
11

12  
13  
14  
15  
16

17               1 State Key Laboratory of Severe Weather, Chinese Academy of Meteorological Sciences  
18               Beijing, China 100081

19               2 Institute of Desert Meteorology, CMA (Chinese Meteorological Administration),  
20               Urumqi, China

21               3National Climate Center, Chinese Meteorological Administration,  
22               Beijing, China 100081

23               4 Taklimakan Desert Atmospheric Environment Observation Experimental Station, Tazhong 841000,  
24               China  
25  
26  
27  
28  
29

30       Submitted to *Journal of Meteorological Research*  
31       January 2, 2018

32       Corresponding author:  
33       Dr. Minzhong Wang  
34               Institute of Desert Meteorology,  
35               CMA (Chinese Meteorological Administration),  
36               No. 46, Zhongguancun South Street, Haidian District, Beijing  
37               P. R. China, 100081  
38       Email: [wangmz@idm.cn](mailto:wangmz@idm.cn)  
39               dorn1984@163.com

## Abstract

During the summer season over Taklimakan Desert, the maximum height of the CBL (convective boundary layer) can exceed 5,000 m, which appeared to play critical roles in simulating the regional circulation and weather. In this paper, we use a combination of WRF-LES (Weather Research and Forecasting Model Large-Eddy Simulation), the GPS radiosonde and eddy-covariance station to evaluate the performance of WRF-LES in the deep convective PBL case over the central Taklimakan. Results show that the model reproduces reasonably well the evolution of PBL processes. However, simulations are relative warmer and moister than those observed due to the over-predicted surface fluxes and largescale advection. Tests are further performed with multiple configurations and sensitive experiments. Sensitivity tests to Lateral Boundary Condition(LBC) showed that the model results are very sensitive to changes in time resolution and domain size of Specified LBC. It is found that larger domain size varies the distance of the area of interest from the LBC, is efficient to reduce the influences of large forecast error near the LBC. However, more frequently updated LBC is desirable to inhibit model error near the LBC. On the other hand, model error increased as the distance between the area of interest and the lateral boundaries decreased. Furthermore, comparing model results using the original surface land parameterized sensible heat flux(SH) with Noah land-surface scheme and those of sensitive experiment, it is concluded that the desert CBL is very sensitivity to SH produced by surface land scheme during summer day time. A reduction in SH can correct overestimate of the potential temperature profile. However, increasing SH significantly reduce the total time needed for CBL increase to a relative low altitude (< 3 km) at the middle and preliminary stage of the development of CBL rather than produce higher CBL at the late stage

63    Keyword: WRF, Large Eddy Simulation, Convective Boundary Layer, Taklimakan

64

65

For Review Only

## 1 Introduction

The Taklimakan Desert, locates at the south center of the province of Xinjiang, China, is the world's second-largest flow desert and has profound influences on the regional weather and climate. Because of the extreme near-surface temperatures, the Taklimakan PBL (planetary boundary layer) commonly reaches 4–6 km during boreal summer(Wang et al.), making it probably the deepest on earth. The deep PBL, which is significantly higher than that of the surrounding mountains and oases, appeared to play important roles on regional circulation and weather. In the northwest of china, the ability to accurately forecast in Taklimakan Desert especially the PBL processes is an important problem.

The large desert (such as Sahara, Taklimakan et al.) atmosphere is always a key component of the climate system. The surface heating from intense solar radiation leads to the development of a near-surface thermal low pressure system, commonly referred to as the heat low(Engelstaedter et al. 2015). However, despite of the vital role of the desert playing in the climate system, observations are extremely sparse, and thin data that exist are mostly from the surrounding of the desert due to the poor work and natural(Marsham et al. 2011). This fundamentally restrict the development of understanding desert and surrounding area, and leads to large discrepancies to analyses and significant biases in operational numerical weather prediction (NWP) models, given the scarcity of observation being assimilated by operational systems. The ability of these local models to simulate real-world cases is often hindered by a lack of favorable data needed to assess the performance of model results(Garcia-Carreras et al. 2015). To fill in the gaps of Taklimakan desert, the field observation experiment was held during the month of July 2016 in Tazhong, which is located

88 at center of Taklimakan, by the Institute of Desert Meteorology (IDM), Chinese  
89 Meteorological Administration (CMA), Urumqi(Liu et al. 2012; WANG et al. 2016a; Wang  
90 et al. 2016b). This will also give the opportunity to evaluate the performance of the deep PBL  
91 process in NWP models over Taklimakan.

92 On the other hand, atmospheric motions interweave small-scale, complex and multiscale  
93 nonlinear interactions. Due to the limited resolution (time and space) mesoscale atmospheric  
94 models are still unable to explicitly represent all these processes(Talbot et al. 2012). Such  
95 processes include turbulent motions, which are too small-scale to be explicitly resolved in the  
96 atmospheric model by a simplified process. Furthermore, turbulent mixing throughout the  
97 PBL can heavily impacted NWP forecasting (Shin; Hong 2011; Shin; Hong 2015).

98 One way to tackle complex turbulent flows in weather forecast models is Large eddy  
99 simulation (LES) which explicitly resolve energy-containing turbulent motions that are  
100 responsible for most of the turbulent transport(Moeng et al. 2007). It has been used  
101 intensively to examine detailed turbulence structure, to generate statistics, and to perform  
102 physical-process studies(Garcia-Carreras et al. 2015; Heinold et al. 2013; Heinold et al. 2015;  
103 Heinze et al. 2015; Sun; Xu 2009). However, most LES applications to the PBL have been  
104 limited to idealized physical conditions. Recently, some studies attempt to test LES and assess  
105 its performance in simulating real cases(Liu et al. 2011; Talbot et al. 2012). Liu et al. (2011)  
106 suggests that WRF-LES is a valuable tool for simulating real world microscale weather flows  
107 and for development of future real-time forecasting system, although further LES modeling  
108 tests, such as elucidate whether inaccurate synoptic forcing or coarse resolution, are highly  
109 recommended. Talbot et al. (2012) suggested that the ability of WRF-LES to simulate

real-world cases are hindered by a lack of favorable synoptic forcing. The initial(ICS) and lateral boundary conditions(LBCS) was found to be more critical to the LES results than subgrid-scale turbulence closures. Thus, the LBCS of can significantly alter high-resolution LES status through inflow boundaries(Rai et al. 2017).

However, most of research above on LES over desert has been limited to idealized physical conditions(Garcia-Carreras et al. 2015) or conducted real case outside Taklimakan(Liu et al. 2011; Talbot et al. 2012). The aim of this study is the attempt to applicate LES in a real deep CBL case over Taklimakan. An important aspect of the ongoing this paper is to examine assess the skillfulness of WRF-LES in relative coarse resolution (333m) over Taklimakan dessert in simulating real cases of deep desert PBL process during boreal summer events in Taklimakan. First we use a combination of WRF-LES and the GPS radiosonde and surface fluxes calculated by an eddy-covariance method taken in the central Taklimakan to evaluate the performance of WRF-LES in real case. Then we assess the potential errors related to LBC. Moreover, we aim to evaluate the relative contribution of uncertainties in surface model to the typical behavior of PBL processes by conducting the sensitivity experiments. Thus, the sensitivity of the performance to surface sensible heat flux (SH) is also studied. Section 2 gives a brief description of synoptic of the study case, and we described data and model configuration and design of numerical experiments used in this study. We presented the results of numerical simulations in Section 4. Finally, we summarize conclusions in Section 5.

## 2 Method

### 2.1 Model configuration

The WRF model of version 3.8.1 (Skamarock et al. 2008) is utilized here at sub-kilometer resolutions to simulate the extreme CBL event in Taklimakan desert. The model is integrated for 12h, starting from 0800 **BJT (Beijing Time)** 01 Jul 2016. We conducted one-way nest WRF from mesoscale down to LES-scales. All domains were 51 levels extended to 50 hPa. **Height for lowest 20 levels are 1130.473, 1157.705, 1207.765, 1294.703, 1423.873, 1591.895, 1795.526, 2021.868, 2272.33, 2558.433, 2882.675, 3248.113, 3658.499, 4118.481, 4633.882, 5212.111, 5855.802, 6517.111, 7151.295, 7757.151.** The model horizontal spacing is 12km 3km 1km and 0.33km for d01 d02 d03 and d04. The sizes of model grids are 411 ×321 791x651 211x201 and 403x406 respectively. Figure 1 shows the domain for all experiments **except for BDY\_T3. Smaller grid sizes (205 X 208) are used in experiment BDY\_T3 to verify the effect of domain size on LES simulation.**

The initialized condition and lateral boundary conditions are provided to the coarsest mesoscale simulations from NCEP Global Data Assimilation System (GDAS) Final Operational Global Analyses. The analyses are 0.25-degree by 0.25-degree grids prepared operationally every six hours and available on the surface, at 32 mandatory (and other pressure) levels from 1000 millibars to 10 millibars (National Centers for Environmental Prediction 2015).

The model physical options include the WSM5 microphysics scheme (Hong; Lim 2006), the Yonsei University (YSU) planetary boundary layer scheme (Hong; Pan 1996), the Kain–Fritsch cumulus parameterization scheme (Kain 1993; Kain 2004), **RUC (Rapid Update Cycle) land-surface model** (Smirnova Tatiana et al. 2000; Smirnova et al. 1997), the Rapid Radiative Transfer Model (Mlawer et al. 1997) longwave, and the Dudhia shortwave radiation scheme



(Dudhia 1989). The cumulus parameterization scheme is only applied to the d01(12km) grid domain to parameterize the convective rainfall. While, the large-eddy-simulation (LES) is only applied to d04(0.333km).

Table 1 shows the list of experiments. Experiment 1 was the control experiment, denoted as CTRL. The experiment 2 (6-hour update LBC, denoted BDY\_T2) and experiments 3(with domain sizes 205 X 208, denoted BDY\_T2) were conducted the same as CTRL with different domain sizes and LBC update frequency. In experiment 4 (denoted HFX\_%75) and 5 (denoted HFX\_%125), the SH (sensible heat flux) was reduced to 75% and 125% of that in the control experiment in the RUC land-surface scheme, to highlight the impact of SH on deep CBL at Taklimakan desert, respectively. In experiment 6 (denoted Noah), Noah land-surface model(Chen; Dudhia 2001a, 2001b) was used to replace the RUC land-surface model in CTRL experiment to discriminate the influence of different land-surface model on deep CBL.

## 2.2 Data

The model simulations are compared to the Tazhong field experiment, which was held during the whole month of July 2016 in Tazhong, by the Institute of Desert Meteorology (IDM), Chinese Meteorological Administration (CMA), Urumqi. The main station was located at 86.63° E, 39.03° N. The location is relatively flat with few hills and covered by sand combined with grass (Figure 1), and the deep PBL of our simulation was under a cloudless sky and dry environment. Instruments are described as follows:

1) surface fluxes: The eddy correlation system was a R3-50 supersonic anemometer developed by Gill Company, UK, deployed at a height of 10 m. The data acquisition

frequency was 20 Hz, and the surface sensible heat flux was calculated by the eddy-covariance method.

2) vertical profiles measured using soundings: Upper air soundings of temperature, pressure, humidity, and wind speed and direction were conducted 3-6 times per day with the GPS sounding system developed by No. 23 Institute of China Aerospace Science & Industry Corp. (CASIC23). The sounding times were 01:15, 07:15, 10:15, 13:15, 16:15 and 19:15 respectively.

### 2.3 Synoptic

Figure 2 shows the synoptic patterns at 0800 BJT 1 July 2016 at 850 700 500 and 100 hPa. There were cyclonic vortex from 850 to 500 hPa center at  $55^{\circ}$  N (Figure 2a ,b and c). Taklimakan was located east of cyclonic vortex and embedded in east–west–elongated ridge at 0800 BJT 1 July. To the southwest, influenced by the South Asia High, which was centered over the eastern Iranian Plateau, the upper air over the Taklimakan Desert was controlled by the westerly jet stream at 100hPa (Figure 2 d). The low-pressure system at low level, which is termed of heat low (Figure 3), dominated most area of southern Xinjiang and resulted in continuous high temperature over the desert. This situation favored the subsidence motion and served as a triggering mechanism for deep PBL in the region in the coming 2–3 days (not show).

## 3 Results

### 3.1 Validation of the deep CBL structure

Time series of surface variables at Tazhong station from CTRL simulation for 01 July 2016 are presented in Figure 4a, b. Results show that discrepancies of thermodynamic surface

variables (the surface temperature, sensible and latent fluxes) between model and observation are large during simulation. The SH (surface sensible heat flux) is far less in observation (maximum:  $243 \text{ W m}^{-2}$ ) relative to model (maximum:  $613 \text{ W m}^{-2}$ ). This represents SH from WRF simulation is 2.5 times than that of observation when both of which reach its maximum. On the other hand, model shows a significant cold bias for the surface temperature. The surface temperature is much higher in observation (maximum:  $70^\circ\text{C}$ ) relative to model (maximum:  $50^\circ\text{C}$ ). To further verification the surface variables, RMSE (root mean squared error) and BIAS (mean bias) are calculated including integration hours from 3 to 12 h for Tazhong station in Table 2. As mentioned earlier, model show yields significantly overestimate of SH (RMSE  $263.636 \text{ W/m}^2$ , BIAS:  $250.14 \text{ W/m}^2$ ) and dramatically underestimated of surface temperature (RMSE  $14.65^\circ\text{C}$ , BIAS:  $-13.37^\circ\text{C}$ ).

Two possible reasons result in model SH far above that of observation: (1) The mismatches of land-use between the model and the observation. WRF use land-use categories to assign certain static parameters and initial values to each grid cell, for example, albedo, surface roughness, and so on (Schicker et al. 2016). However, As in Figure 1c, the EC station is surround by mixing land of grass and sand. The complex underlying surface may not be adequately reproduced by model and can have an impact on the overestimate of SH in this case. (2) It is should be noted that the SH and LH (latent heat flux) based on eddy correlation might be underestimated (LeMone et al. 2013). Researchers found that if the other two terms in the budget—net radiation and flux into the soil were accurate, used data for the whole experiment to find the  $H + LE$  for Tazhong station are equal to an average of 75% of what would be required for balancing the surface energy budget.

Despite the large differences on surface, near-surface variables (2m temperature, relative humidity and 10m wind speed, Figure 4 e f g) are closer to measurements than those from surface, their values are relatively higher than those observed. The time series evolution of 2m temperatures nearly follow those of the observations (RMSE:1.66, BIAS:1.61); but model produce warmer surfaces by about 3 K at the beginning of model integration, and 1K when model and observation both reach their maximum temperature, respectively.

Results indicate that, model-produced near-surface relative humidity is close to observations at initial time (Figure 4 f). However, the humidity from the model keeps increasing at the first few hours of model integration, when observations decrease. After 3 hours' spin-up, the model reproduces reasonably well the evolution of humidity, in agreement with observation (RMSE:1.22), but their values are relative higher than those observed (BIAS:1.11).

One reason for this discrepancy is the overestimate of soil moisture during simulation. Soil moisture can severely impact near-surface humidity. The overestimate of the soil moisture contents in the initial condition of the model, which are only offered to the model at initial time, may result in considerable differences in near-surface layer humidity (Talbot et al. 2012). In the present simulations, model results are reported to produce grossly overestimate soil moisture. At the model initialization for the CTRL simulation, EC station at Tazhong station indicated a value of the 5-cm-deep soil moisture of  $0.230 \text{ m}^3/\text{m}^3$ , while the model initial value is  $0.6 \text{ m}^3/\text{m}^3$  (Figure 4 d). This large overestimate of soil moisture results in LH (Figure 4 b, f) from the model continue to increase. As a result, near-surface of model is far moister than that of observation at the first few hours of model integration. An interesting

result to note is that the model simulation has the abilities to correct some of the bias due to the initial condition of the surface; The results from CTRL experiment are closer to observation after 3 hours' spin-up.

The model simulated potential temperature are compared to GPS sounding measurements at Tazhong during 0800~2000 BJT 01JULY2016 in Figure 5 (solid lines). One should note that radio-sounder floating about 7 Km away from Tazhong, when radio-sounder reach 6 Km height. Thus, for comparison, the profiles of model simulations are averaged station in a radius of 3.5 Km. At 0800 BJT, when the model is initialized, the nocturnal inversion reaches 300m (not shown). By 1100 BJT, this inversion is eroded in the model in agreement with observations, and both reaching about 300m at 1100 BJT (Figure 5 a). However, the simulated CBL grows faster in the morning due to larger SH than observation, reaching 3500m (3000m in the observations) at 1400 BJT (Figure 5 b). At 1700 BJT (Figure 5 c), the simulated and observed CBL heights exceed 4000m and 5000m respectively. This indicates that the simulated CBL grows more slowly in the afternoon than measurement. Compared to measurements, the model is initially cooler with faster heating rate in the morning. As a result, model is warmer than measurements in the afternoon. Eventually, model agrees with observations at the end of the day. One possible minor reason is the differences of potential temperature lapse rate above the top of mixing layer between observation and simulation. Simulated stronger inversion layer restrain the development of CBL, which will be discussed below.

Moreover, in terms of CBL temperatures, the model initially simulates a cooler and drier CBL than that observed, at 1100 BJT 01 JUL (Figure 5a). Compared to the observed potential

temperature profile, the CBL seems to appear earlier in model forecasts result based on obvious warming in surface layer. One should note that RL (residual layer) may play a key role in the deep PBL at Taklimakan desert. At 1100 BJT, when the CBLH was about 300 m in observation as show above, potential temperature in the were about 317 in PBL and 320 K in RL, respectively. When the potential temperature in CBL increased to the value in RL (320 K), the CBL merged with the RL, and the height of PBL reach 3000m in the observations at 1400 BJT. These results are in good agreement with Han et al. (2012). By analysis of observation of a CBL in the Badanjilin region, they found a rapid development process of CBL after 1200 LST, which appeared to be a jump of CBLH when the inversion layer vanished.

When the SH reaches its maximum at 1400 BJT (Figure 5b), potential temperature profile is closer to measurements than at initial time, and their values are higher than those observed. By 2000 BJT (Figure 5d), CBLH in the model reaches its maximum value, which is consistent with observation, despite of approximately 0.4K cooler on the lower levels(<2.5Km). As mentioned, one cause of the higher temperatures produced with model would be the large difference in the surface heat fluxes. It was concluded that the surface sensible heat flux from the land surface parameterization is the crucial factor affecting the CBL process during summer day time. Differences in surface SH would create differences in the vertical development of the PBL. Thus, the large surface SH difference between the model and observation may lead to differences in CBL growth during daytime and in its peak depth during the simulation. Fortunately, one can artificially modify the surface SH computed by surface-land model, which

controls the calculation of surface fluxes. Sensitive simulations will be realized and discussed in next section.

Figure 5 also shows Vertical profiles of vapor mixing ratio (dash lines) at Tazhong station. The simulated profiles with lower RL are much drier than observation from 1500 to 3500m at 1100 BJT. The vertical mixing results in the uniform structure of vapor mixing ratio within CBL, so the differences between simulated and observational profiles are reduced remarkably when CBL reach above 4000m at 1400 BJT. Differences are generally less than 1g/Kg at 1100 BJT reaching a maximum of 0.3g/Kg at 1400 BJT. However, measured PBL moisture shows an inverse layer at lower PBL( $\leq 2000$ m) range from 2.8 to 3.6 g/Kg, which is not captured by model. Furthermore, as the convective boundary layer grows, the inversion moisture structure below 3000m develops to and maintains below 3000m during 1400~2000 BJT. By the end of the day, the model-simulated CBL humidity show moister than observation, because model cannot reproduce the inverse moisture layer within CBL.

Inverse humidity may be caused by the joint of the heterogeneous humidity Pattern and Large-scale advection over the underlying surface. For instance, interaction of oasis with desert environment may resulted in the inverse humidity layer in desert PBL. Thus, one possible reason for the discrepancy between model and observation caused by the error in land-use type. The USGS land-use in ARW-WRF is based on AVHRR (Advanced Very High Resolution Radiometer) 1km resolution satellite data during 1992-1993. For our case, this land-use data may be outdated in Taklimakan. Besides such changes, misclassifications are found in the USGS land-use data, the default land-use dataset in WRF(Schicker et al. 2016). This is also confirmed by the discrepancies of land-use between simulation and measured at

the Tazhong station in the previous figure. Large-scale advection of dry air can affect the profile of moisture. Moisture will also be variable in the horizontal, so advection at the low level could contribute to the dry at bottom and moisture at the upper of PBL between 1100 and 2000 BJT at the bottom of the PBL.

The mismatch between the model and the observations in terms of moisture that is present means that the effect of land-use type and Large-scale advection needs to be quantified and that more detailed data of Taklimakan (land and atmosphere) might be necessary to realize a more realistic performance. Extra care should also be taken with sparse and the limited data in the periphery of the Taklimakan (ter Maat et al. 2012).

### 3.2 Sensitive to Lateral Boundary Condition(LBC)

After verifying the details of the LES simulations, we assess the sensitivity of the LES simulations to time resolution and domain size of Specified LBC. For one-way nest, Specified LBC is obtained from coarser model simulation. The analysis and all forecast times from a previously-run larger-area model simulation are used to specify the LBC. The primary cause of differences in PBL structure was diagnosed as differences in domain size and frequency provided by the coarser resolution. The aim is to assess the sensitivity of the finer large-eddy simulations to time frequency and domain size of Specified LBC forcing by larger-area model simulation; Details of the three simulations (CTRL, BDY\_T2 and BDY\_T3) are given in section 2.

Figure 5 compare the profiles of the simulated potential temperature and vapor mixing ratio profiles from LBC sensitivity experiments and observation. Results indicate that, there is a distinct relationship between LBC and CBL development. All model-produced profiles are



nearly the same at initial time (not show). However, the comparison results reveal that discrepancies among different experiments are large for CBL. The results indicate that larger domain size and more time frequency LBC leads to a warmer and drier PBL, but a cooler and moister free troposphere. Such sensitivity is monotonic with respect to LBC (Figure 5). Furthermore, in the next three hours, the differences between the sensitive experiments keep increasing with time (Figure 5 a, b). The potential temperature profiles within CBL become divergence at 1100 BJT. However, the results show more convergence at afternoon as CBL continues to grow (Figure 5 c). Finally, largest discrepancies are found by end of the day (Figure 5 d) where the model CBL potential temperature is warmer by up to about 0.7K and 0.9K in BDY\_T2 and BDY\_T1 respectively, compared to measurements.

Figure 6 shows cross sections along 39.03°N of horizontal winds, superposed with theta and vapor mixing ratio. Overall, the **lower** frequently updated LBC is desirable to cold zone near the LBC, which results in cold advection of the temperature and moisture to the area of interest (Figure 6 b, c). Larger domain size, which varies the distance of the area of interest from the LBC, is efficient to reduce the influences of large forecast error near the LBC to the area of interest (CMP Figure 6 a, c). The results suggest that the model results are sensitive to changes in time resolution and domain size of Specified LBC. The mismatch among sensitive experiments is present means that the effect of LBC needs to be quantified to realize a more realistic performance in the sub-kilometer simulations.

**To further examine the impact of LBCS on the turbulence of deep Taklimakan desert CBL, the instantaneous vertical velocity fields for the horizontal are displayed in . By 1400 BJT, the convection of CTRL simulation obviously intensified under strong surface heating**

(Xu et al. 2018). Thus, the maximum vertical velocity reaches 9 m/s and the depth of mixed layer grows to about 4.3 km (a). The distances between the boundary layer rolls correspondingly increase to about 12 km and the height of the peak updraughts is raised to just under 4 km. The cellular shape of updraughts and downdraughts characteristic of boundary layer rolls is obvious in the horizontal view with the strength of convection. BDY\_T2 and BDY\_T3 experiments (b, c) both reproduce motions with much weaker maximum and minimum values at boundary of domain. In BDY\_T3 experiment, Tazhong station at center of the model has been directly influenced by the inflow cold advection produced by low frequency LBCS and results in much weaker maximum and minimum value of  $w$  (about 6 m/s). However, despite the underestimate of potential temperature, the  $w$  fields for BDY\_T2 experiment look similar to the CTRL  $w$  in plain view, and the horizontal extent of the updraughts/downdraughts agrees with the CTRL as can be inferred from . To further examine vertical structure of desert CBL, vertical cross-sections along Tazhong station ( $39^{\circ}\text{N}$ ) of  $w$  are presented in Figure 8. Wide and regularly spaced updraughts along A1- A2 split into the stronger and more irregular motions in CTRL and BDY\_T2. The updraughts are much weaker in the BDY\_T3 experiment, as can be seen from Figure 8 c. Peak updraughts on BDY\_T3 are about 4 m/s much weaker than on CTRL (9 m/s) and BDY\_T2 (8 m/s). For BDY\_T2 and BDY\_T3, the distant of the inflow boundary is wider, and the intensity of the convection is weaker at the boundary. Compared with BDY\_T2, the horizontal distribution of vertical velocity at Tazhong station in BDY\_T3 experiments is much weaker.

### 3.3 Simulations with different surface sensible heat flux (SH) and surface-land models

The import cause of differences in PBL structure was diagnosed above as differences in SH predicted by the surface-land schemes. The SH is one of the key factor affecting the CBLH during summer day time. Thus, the difference between model and observation may lead to differences in PBL growth during daytime; To further confirm whether this indeed occurs, **three** additional sensitive simulations were realized based on the CTRL experiment. **For Noah experiment Noah land-surface model is used to replace RUC land-surface model in CTRL experiment, and for HFX-125%, HFX -75% SH is %125 and %75 that of CTRL (HFX -100%) experiment, while the other parameters remain the same.**

The results **from Figure 10** and Table 2 showed that HFX-75% successively improved the simulation of SH with RMSE:151.12, compared that of 263.64, 357.11 in CTRL and HFX-125%. Of interesting is that experiment with Noah surface-land yielded the best performance among all of the cases in SH, surface temperature and air temperature. However, Noah surface-land model show large discrepancies with observation in Soil moisture, and results in dramatically overestimate of LH and relative humidity compared to CTRL.

Further examining potential temperature and vapor mixing ratio (**Figure 9**) indicate that with smaller SH leads to a cooler, moister lower PBL and a warmer, drier free atmosphere. Such sensitivity is monotonic with respect to SH. Overall, the CBL structure from the HFX-75% **and Noah experiments match** the GPS measurements better than the CTRL (HFX-100%) simulations. Potential temperature profiles from CTRL (HFX-100%) and HFX-125% are consistently warmer than the observation by about 0.4 and 0.5 K respectively, while results from **HFX-75% and Noah** are within about 0.2K at 1400 BJT (**Figure 9 b**). The results suggest that the model results are sensitive to changes SH from land-surface model.

However, simulations converge at the end of the day, but remain differences at 2000 BJT (Figure 9 d). HFX-75% and Noah with weaker surface sensible heat flux can still produce the deep CBL nearly the same as CTRL and HFX-125%. This indicates that SH may not the dominant factor for the deep CBL over the Taklimakan desert.

Results of simulations on desert PBL in the morning agree with the previous studies of sensitivities land-surface model for other areas (Hu et al. 2010; Zhang et al. 2017). However, during 1700~2000 BJT 01July (Figure 9b, d), all experiments produce nearly the same CBLH and moisture in agreement with observation in the PBL. The effects of SH on the evolution of Taklimakan PBL structures during this period are needed to be further examined and discussed. So, the question is: why are simulations insensitive to land-surface process by the end of the day? As in Stull (1988), the development of CBL is mainly influenced by the effect of thermodynamic and turbulent entrainment without considering large scale factors such as large scale advection or subsidence. Besides the surface sensible heat, the intensity of entrainment process determines the increasing rate of CBL. Thus, the entrainment rate  $w_e$  is a valuable indicator for the development of PBL structure.

The rate of growth of the convective boundary layer is mainly determined by the entrainment rate  $w_e$  at the inversion layer without considering large scale vertical motion.  $w_e$  usually has a positive correlation with heat flux amount at the inversion layer  $\overline{(w'\theta_v')_h}$ , and large LES experiments show  $\overline{(w'\theta_v')_h}$  is about 0.2 times the surface flux of buoyancy  $\overline{(w'\theta_0')}$ . During the period from 1100 to 1400 BJT, larger SH is obviously correlated with stronger turbulent entrainment and warmer air from free atmosphere (FA) entraining into ML. As a result, CBL develop rapidly and is warm too fast in the early simulation phase due to the

obviously increasing temperature and strong vertical mixing in model. Of interesting is that reduction in SH reproduces better desert PBL evolution in the early simulation phase, as SH-75% and Noah produce the smallest simulation errors in both temperature and moisture. However, one should note that CBLH and potential temperature for SH-75% and Noah have reached above 5000 m and 323.2 K respectively at 1700 BJT (Figure 9 a). For the rest of the day, the increase rate of CBL height slows down due to the deep CBL(>5000m) which require more heat for the growth of PBL depth; Moreover,  $w_e$  decrease with increasing inversion intensity, which inhibits the mixing and entrainment processes. These two factors obviously limit the growth of CBL when CBLH is over 5000 m in this deep desert CBL case. Therefore, increasing SH from 75% to 125% significantly reduce the total time needed for CBL increase to a relative low altitude (< 5 km) at the middle and preliminary stage of the development of CBL rather than produce higher CBL at the late stage. When height of CBL over Taklimakan desert exceeds 5000 m, it might not change with proportion to SH fluxes (Figure 9 d). As a result, PBL of WRF simulations are basically the same, and not sensitive to SH fluxes by the end of the day.

#### 4 Summary

This paper assesses the performance of the Weather Research and Forecasting Model (WRF) Large-Eddy Simulations(LES) in deep convective PBL case over Taklimakan Desert. Tests are performed with multiple configurations and sensitive experiments. Sensitivity tests to Lateral Boundary Condition(LBC) showed that the model results are sensitive to changes in time resolution and domain size of Specified LBC. It is found that larger domain size varies the distance of the area of interest from the LBC, is efficient to reduce the influences of large

440 forecast error near the LBC.

441       Consequently, with the configuration used in this study, the model reproduces  
442 reasonably well the evolution of PBL processes. The model shows discrepancies between the  
443 main CBL characteristics in the morning including the thermal and moisture structure. The  
444 model simulates the relatively colder and drier morning CBL well, underestimating it by up to  
445 1.5K near-surface layer at Tazhong station. In the case of the underestimation of moisture by  
446 only up to 1 g/kg in the near-surface layer. The overestimation of CBL profile may be caused  
447 by discrepancy between model and measurement initially. This indicates that the results are  
448 sensitive to the model initial conditions. An interesting result to note is that the model  
449 simulation seems to be able to correct some of the bias due to the initial condition. In the  
450 afternoon, the model correctly reproduce the thermal structure, but simulations are relative  
451 warmer and moister than those observed. Potential temperature profile at CBL appears  
452 warmer by up to about 0.4K compared to the observations. While the model overestimates the  
453 afternoon moisture seriously, it mainly overestimates vapor mixing ratio by about 1 to 2 g/Kg  
454 in the CBL. Largest discrepancies are found in 0~3Km where the model vapor is twice as  
455 moist (up to about 3g/Kg above AGL) as observed.

456       Furthermore, three additional sensitive simulations were realized to further confirm  
457 whether large differences of SH lead to differences in ABL growth during daytime, based on  
458 the CTRL experiment. The results suggest that the model results are sensitive to changes  
459 SH and different land-surface models. The large difference between the model and  
460 observation may lead to differences in CBL growth during daytime. From these results, it was  
461 concluded the surface sensible heat flux is an important factor affecting the CBL depth over

Taklimakan during summer day time. However, its peak depth during the simulation show less sensitive to SH because of decreasing  $w_e$  by the end of the day.

The future work aimed to study several other deep CBL cases over Taklimakan to summarize their common features. Furthermore, we hope to utilize high resolution model and observation to describe the fine characteristics of a typical deep Taklimakan CBL particularly the turbulent and vertical mixing and its impact on regional weather forecast. This research is aimed to improve the understanding of deep CBL over Taklimakan and its influence on regional weather and climate.

#### **Conflict of Interests**

The author declares that there is no conflict of interests regarding the publication of this paper.

#### **Acknowledgments**

This study is supported by the National Natural Science Foundation of China (Grant no. 41575008 and 41775030). The author would like to thank all the reviewers and editors for their professional advice to improve the paper.

477 Captions:

478 Figure 1 Simulation domains used in ARW model with terrain height (shaded, units:m); (b) land  
479 use categories for domain D03 and D04.

480 Figure 2 Horizontal distribution of geopotential height (solid, units: dagpm), wind speed (shaded,  
481 units: knot), and wind barbs from the NCEP FNL analysis at 0800 BJT 1 Jul 2016 at (a)  
482 850 hPa, (c) 700 hPa, (e) 500 hPa, and (d) 100hPa.

483 Figure 3 NCEP FNL 700hPa potential temperature (colors) and mean sea level pressure (white  
484 lines) at 0800 BJT 1 Jul 2016. The black dot shows the location of Tazhong station at  
485 Xingjiang province.

486 Figure 4 Time series of simulated surface variables **from innermost domain of simulations**  
487 **and surface observations at Tazhong station** ( $83.63^{\circ}$  E,  $39.03^{\circ}$  N) initial at 0800  
488 BJT 01July 2016 (a) sensible heat flux ( $\text{W/m}^2$ ), (b) latent heat flux( $\text{W/m}^2$ ), (c) 2-m  
489 temperature ( $^{\circ}\text{C}$ ), (d) surface temperature ( $^{\circ}\text{C}$ ), (e) 2-m Relative Humidity(%) and (f)  
490 10-m wind speed (m/s ) with corresponding observations.

491 Figure 5 Vertical profiles of potential temperature (solid line, units: K) and vapor mixing  
492 ratio(dash line, units: g/Kg)from innermost domain **of simulations and observation of**  
493 **GPS sounding at Tazhong station** ( $83.63^{\circ}$  E,  $39.03^{\circ}$  N) at (a)1100 (b) 1400 (c)  
494 1700 (d) 2000 BJT 01 Jul2016.

495 Figure 6 cross sections along  $39.03^{\circ}\text{N}$  of horizontal winds (barbs, units: m/s), at intervals of 5 m/s,  
496 superposed with theta (shaded, units: K) and vapor mixing ratio(contour, units: g/Kg), from (a)  
497 BDY\_T1, (c) BDY\_T2, (e) BDY\_T3 experiments at1400 BJT 01JUL2016, (b), (d), (f) are the  
498 same as (a), (c), (e), but for 2000 BJT 01JUL2016.

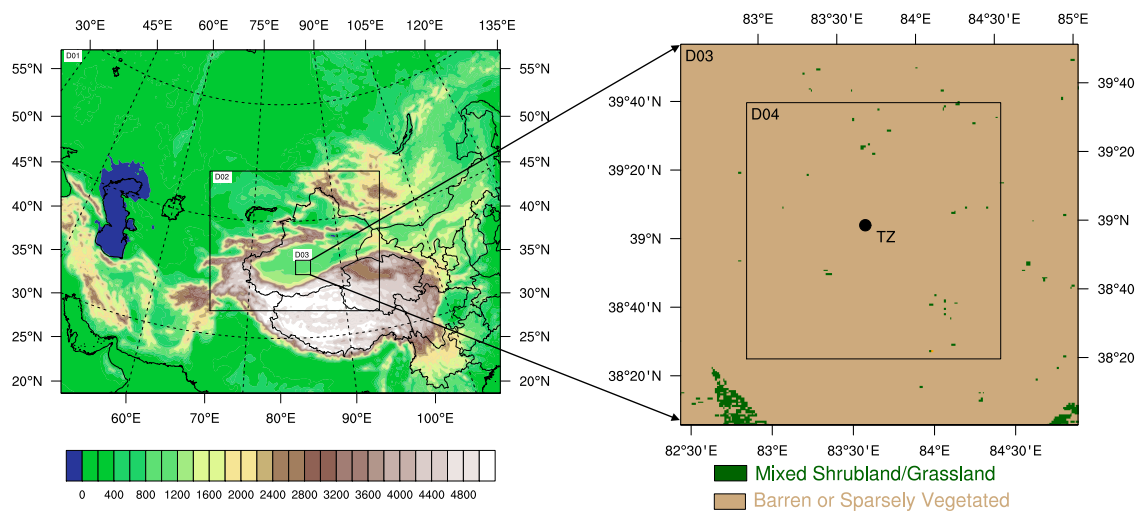


Figure 7 Instantaneous vertical velocity fields (shading: m/s) at 3000 m for (a) BDY\_T1 (CTRL), (b) BDY\_T2, (c) BDY\_T3, and (d) Noah at 1400 BJT, 1 July 2016.

Figure 8 Vertical cross-section of instantaneous vertical velocity fields (shading: m/s) along A1-A2 in for for (a) BDY\_T1 (CTRL), (b) BDY\_T2, (c) BDY\_T3, and (d) Noah at 1400 BJT, 1 July 2016.

Figure 9 The same as Figure 5, but for SH flux sensitive and Noah land-surface experiment.

Figure 10 The same as Figure 4, but for SH flux sensitive and Noah land-surface experiment.



508

509



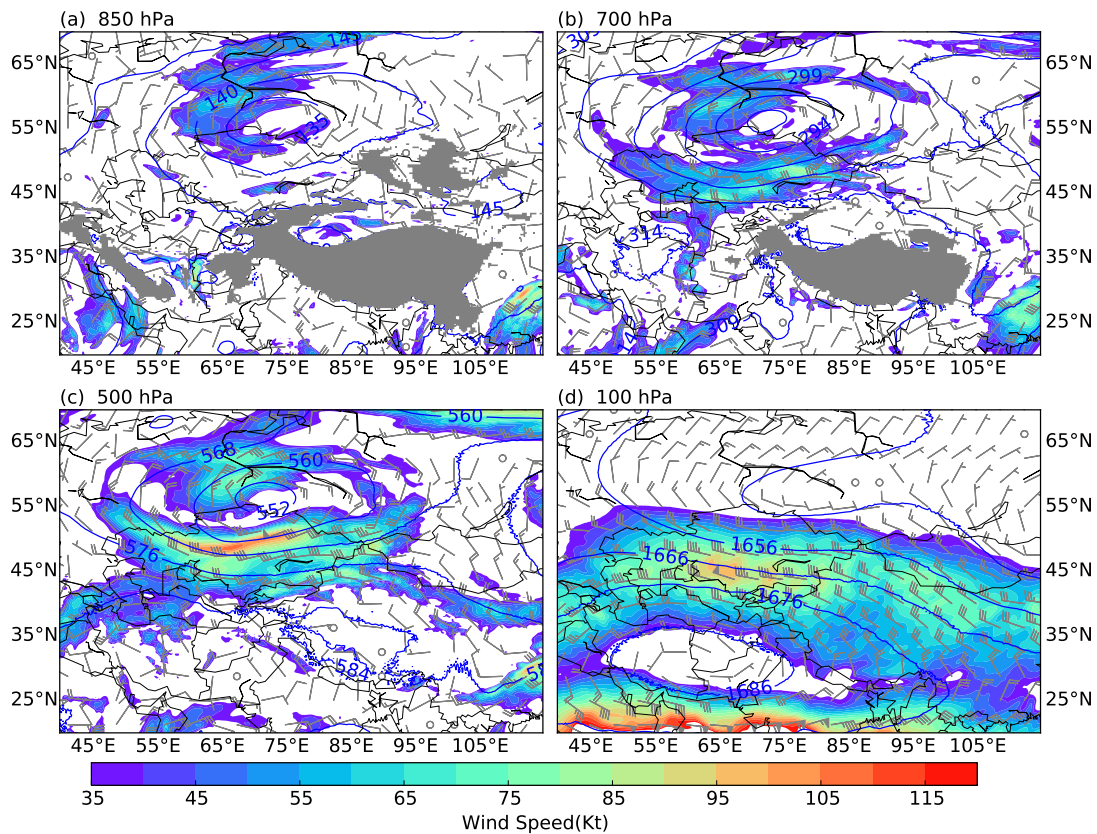
510

511

Figure 1 Simulation domains used in ARW model with terrain height (shaded, units:m); (b) land use categories for domain D03 and D04; (c) photograph of Tazhong station

514

515



516

517 Figure 2 Horizontal distribution of geopotential height (solid, units: dagpm), wind speed  
 518 (shaded, units: knot), and wind barbs from the NCEP FNL analysis at 0800 BJT 1 Jul 2016 at  
 519 (a) 850 hPa, (c) 700 hPa, (e) 500 hPa, and (d) 100hPa.

520

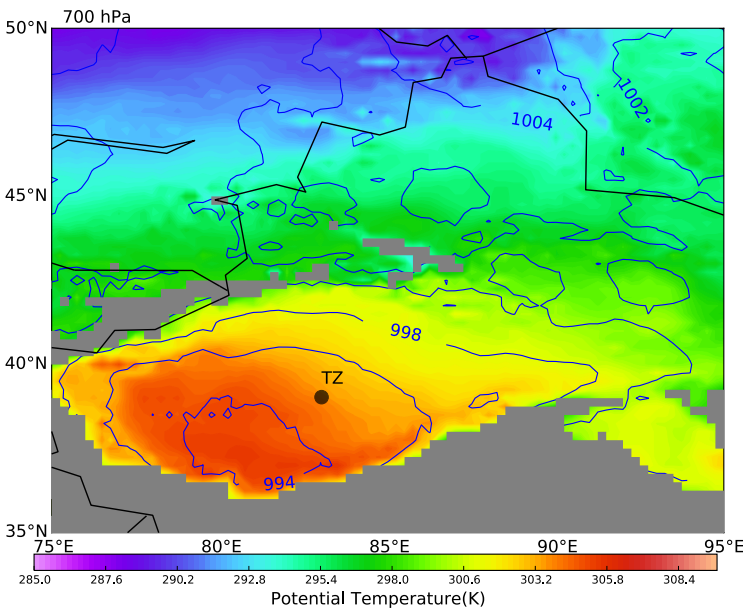


Figure 3 NCEP FNL 700hPa potential temperature (colors) and mean sea level pressure (white lines) at 0800 BJT 1 Jul 2016. The black dot shows the location of Tazhong station at Xingjiang province.

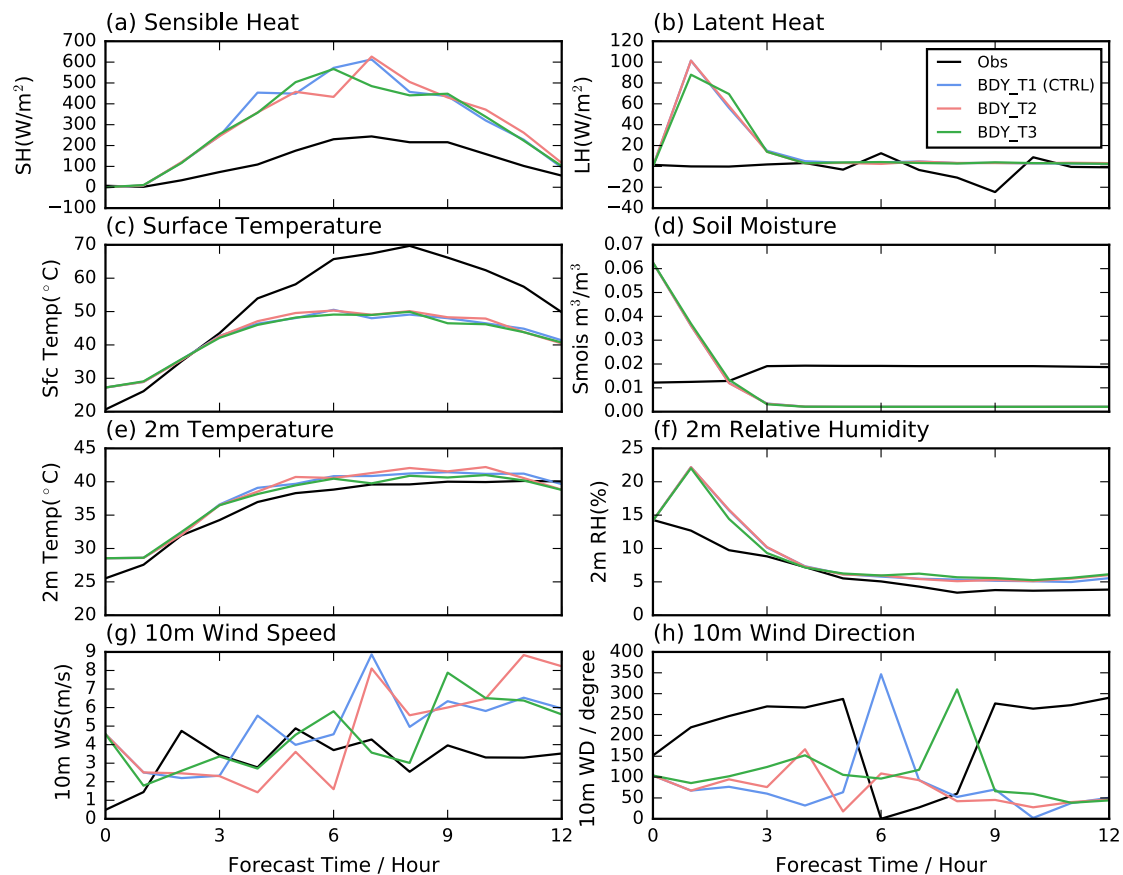


Figure 4 Time series of simulated surface variables from innermost domain of simulations and surface observations at Tazhong station ( $83.63^{\circ}$  E,  $39.03^{\circ}$  N) initial at 0800 BJT 01July 2016 (a) sensible heat flux ( $W/m^2$ ), (b) latent heat flux( $W/m^2$ ), (c) 2-m temperature ( $^{\circ}C$ ), (d) surface temperature ( $^{\circ}C$ ), (e) 2-m Relative Humidity(%) and (f) 10-m wind speed ( $m/s$ ) with corresponding observations.

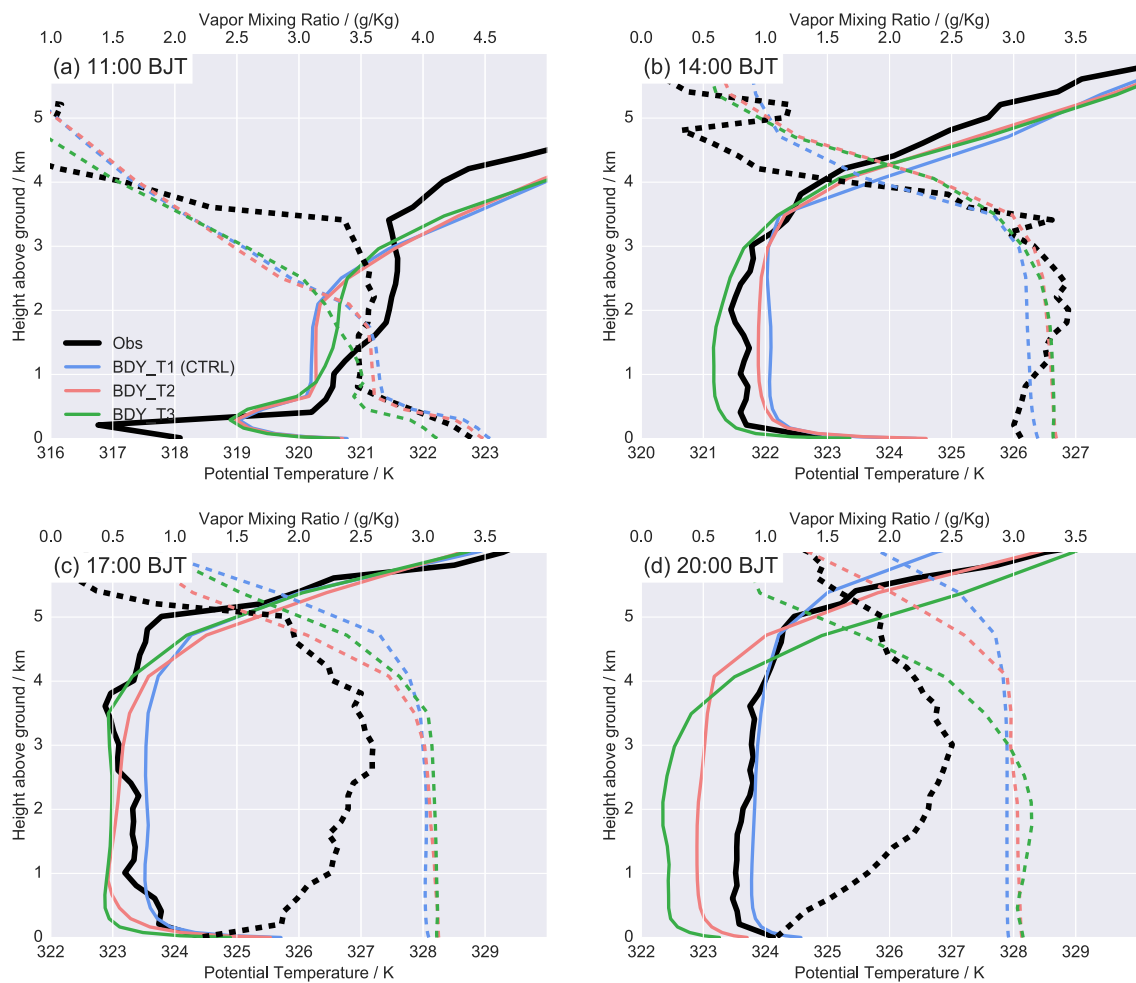


Figure 5 Vertical profiles of potential temperature (solid line, units: K) and vapor mixing ratio(dash line, units: g/Kg)from innermost domain of simulations and observation of GPS sounding at Tazhong station (83.63° E, 39.03° N) at (a)1100 (b) 1400 (c) 1700 (d) 2000 BJT 01 Jul2016. The profile of model output are averaged in a radius of 3.5km.

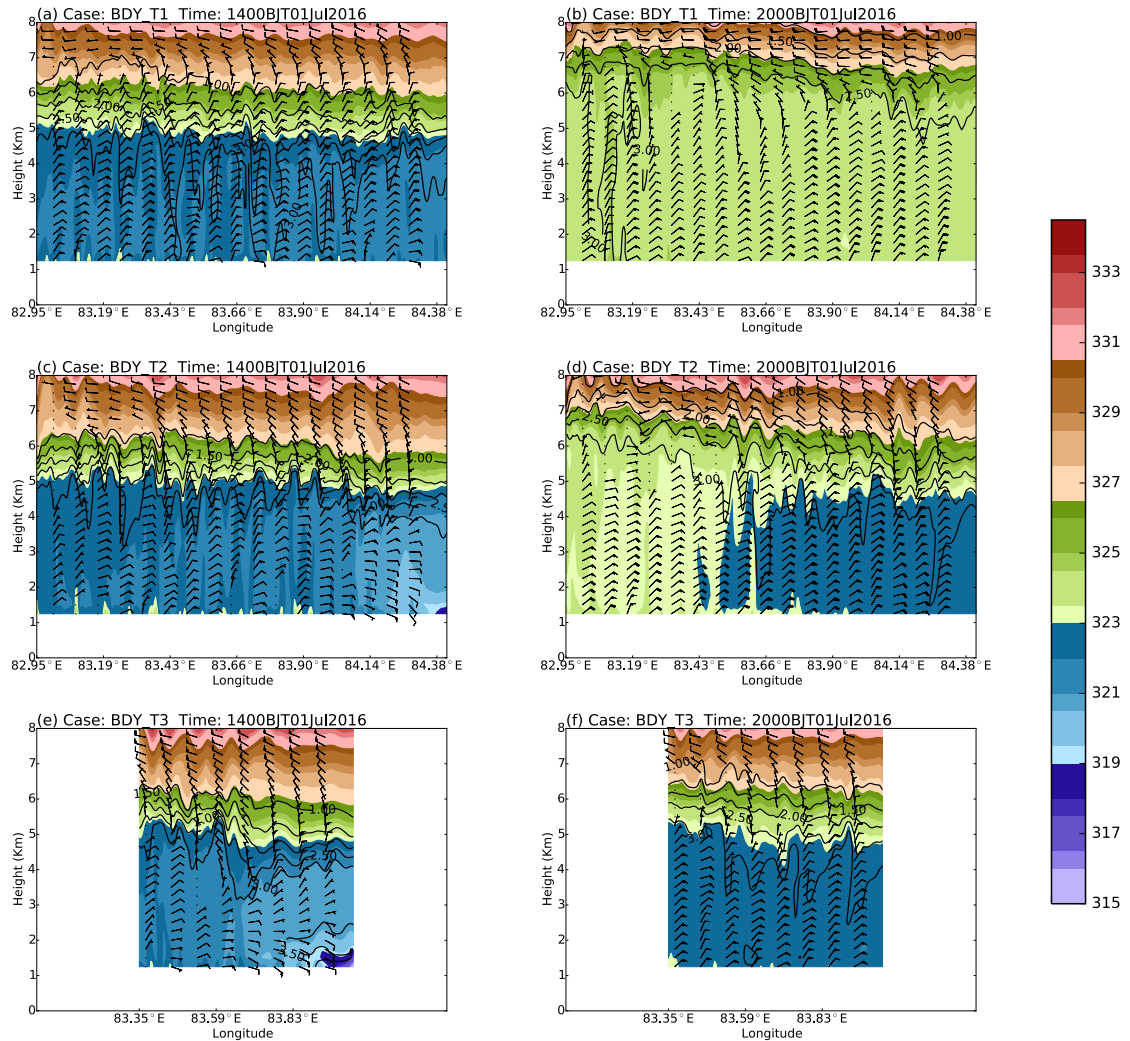
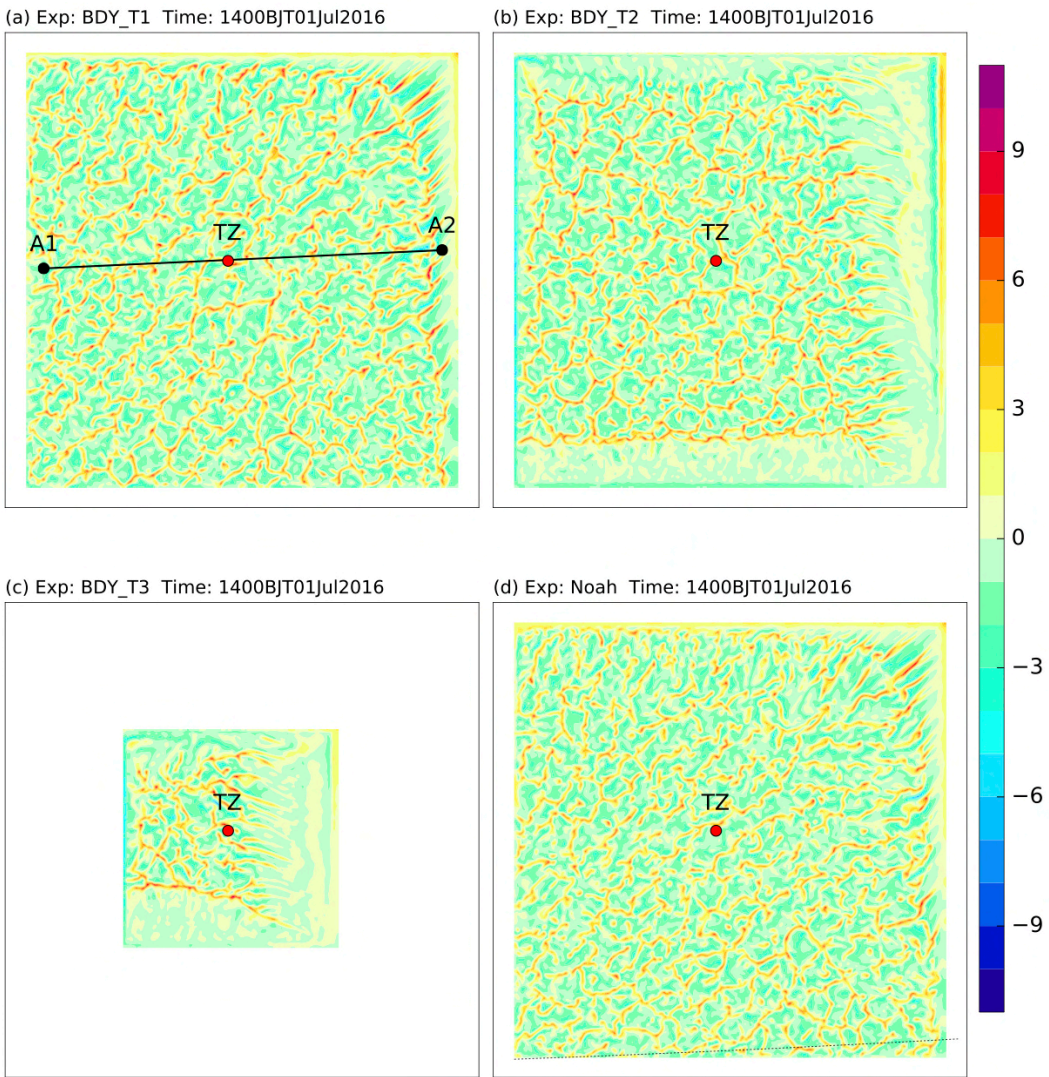


Figure 6 cross sections along 39.03°N of horizontal winds (barbs, units: m/s), at intervals of 5 m/s, superposed with theta (shaded, units: K) and vapor mixing ratio (contour, units: g/Kg), from (a) BDY\_T1, (c) BDY\_T2, (e) BDY\_T3 experiments at 1400 BJT 01JUL2016, (b), (d), (f) are the same as (a), (c), (e), but for 2000 BJT 01JUL2016.



544



545

546 Figure 7 Instantaneous vertical velocity fields (shading: m/s) at 3000 m for (a) BDY\_T1 (CTRL), (b)  
547 BDY\_T2, (c) BDY\_T3, and (d) Noah at 1400 BJT, 1 July 2016.

548



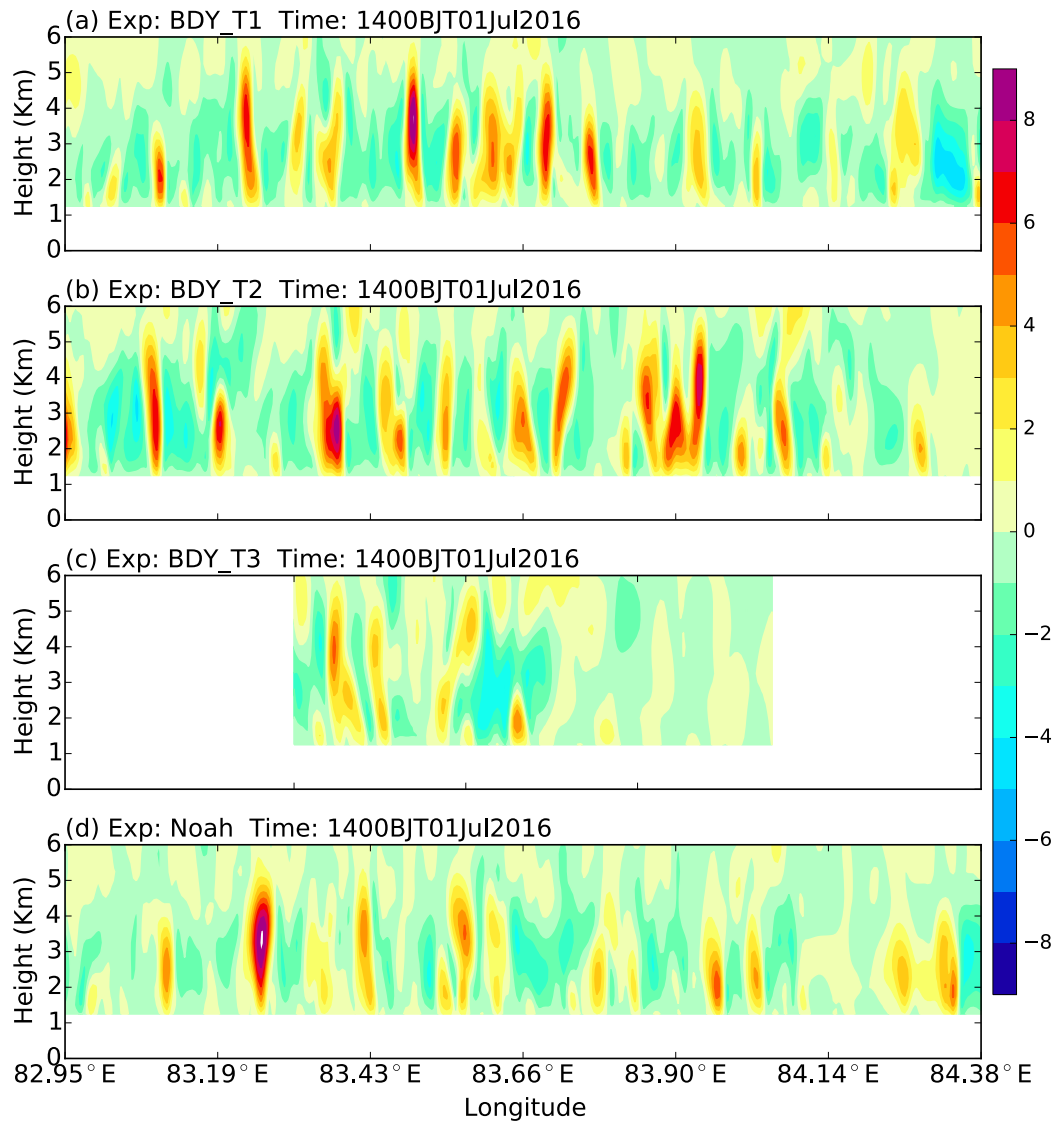
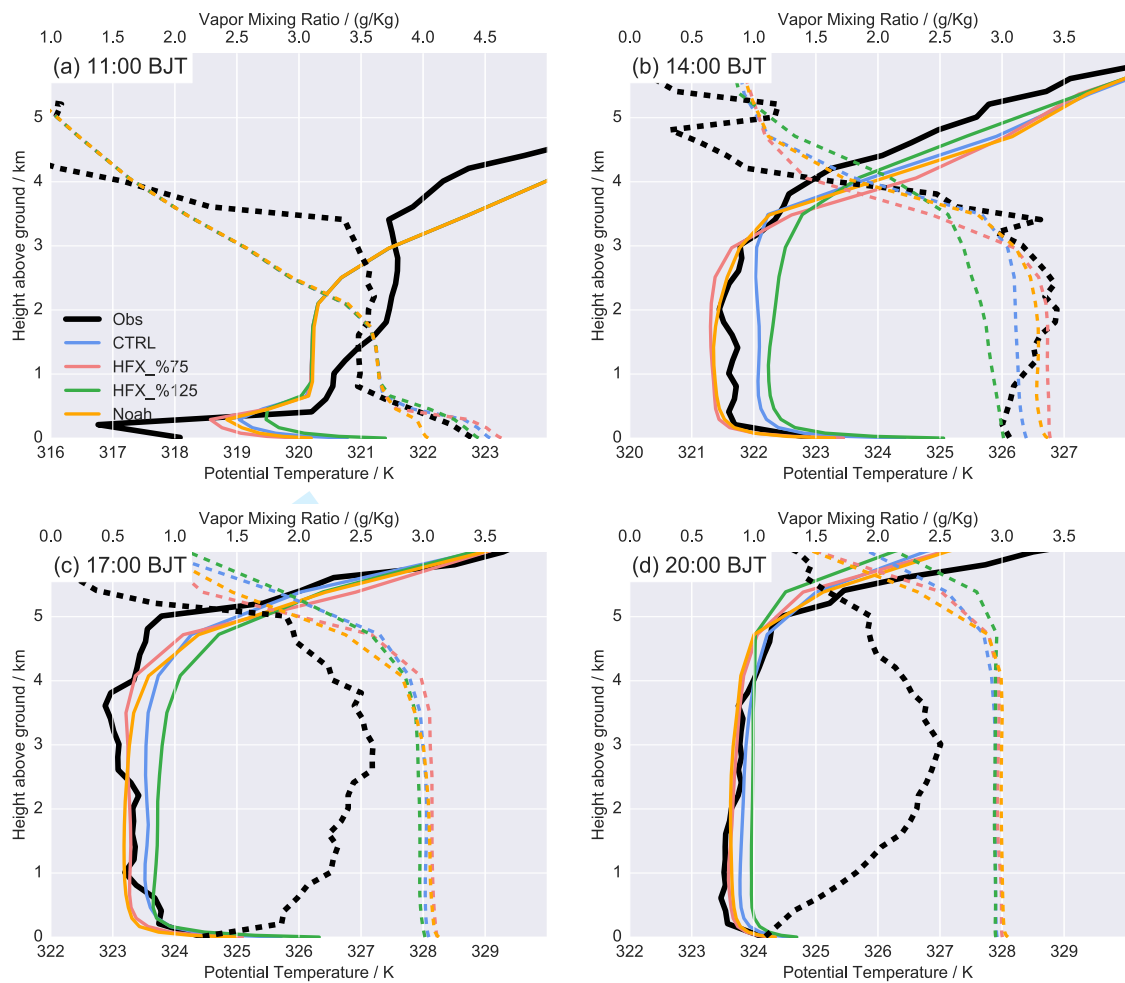


Figure 8 Vertical cross-section of instantaneous vertical velocity fields (shading: m/s) along A1-A2 in for for (a) BDY\_T1 (CTRL), (b) BDY\_T2, (c) BDY\_T3, and (d) Noah at 1400 BJT, 1 July 2016.

555



556

557

558

Figure 9 The same as Figure 5, but for SH flux sensitive and Noah land-surface experiment

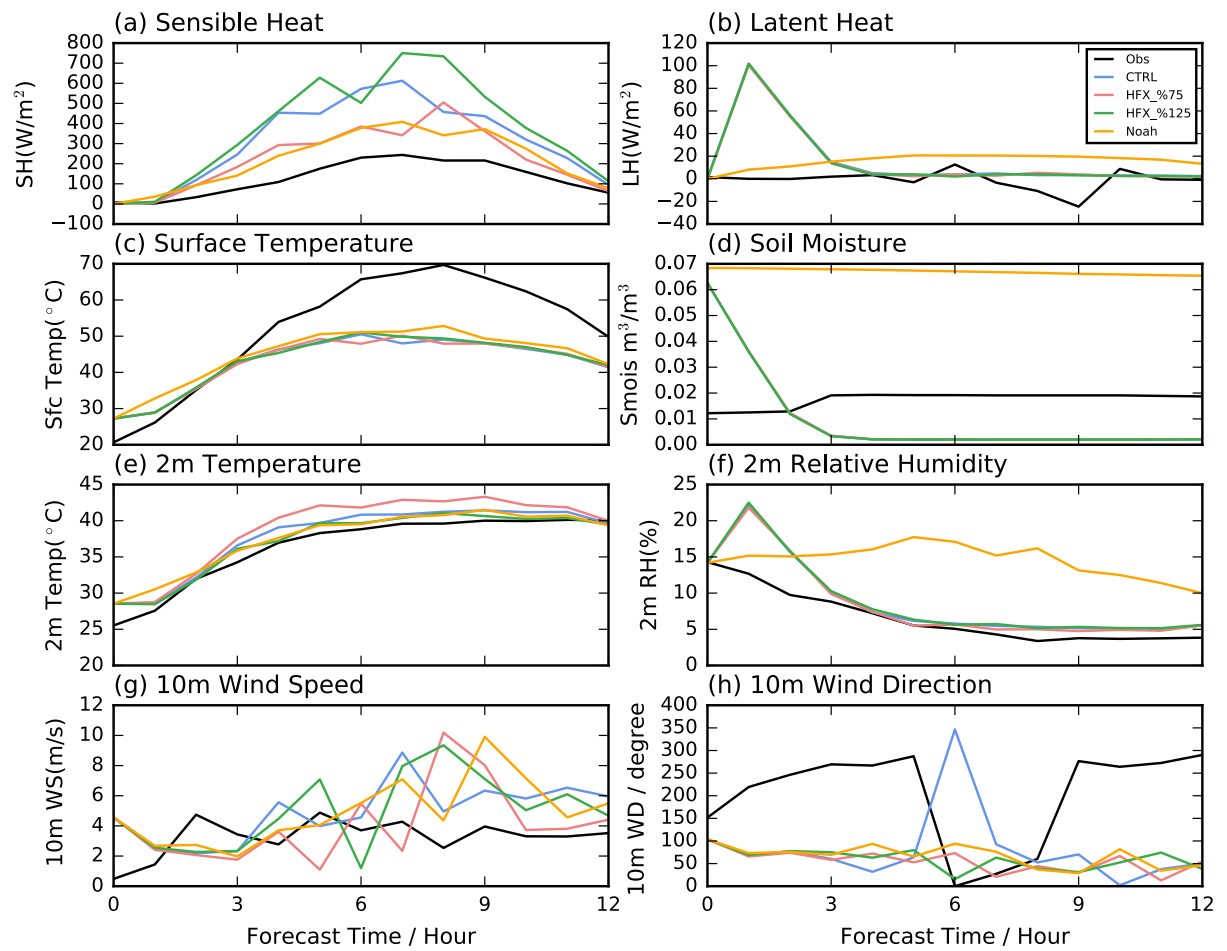


Figure 10 The same as Figure 4, but for SH flux sensitive and Noah land-surface experiment.

562

Experiment	Name	Remarks
1	BDY_T1(CTRL)	LBC of D04 is provide by d03 every 1 hour with model grids 403x406
2	BDY_T2	As BDY_T1, but LBC of D04 is provide by d03 every 6 hour
3	BDY_T3	As BDY_T2, but with model grids 205 x 208.
4	HFX_%75	As CTRL_T2, but with SH 75%.
5	HFX_%125	As CTRL_T2, but with SH 125% .
6	Noah	As CTRL_T2, but with Noah surface-land model.

563

Table 1. List of designed experiments.

564

For Review Only

565

Variables	Sensible Heat		Latent Heat		Surface Temperature		Soil Moisture		2m Temperature		2m Relative Humidity		10m Wind Speed	
	RMSE	BIAS	RMSE	BIAS	RMSE	BIAS	RMSE	BIAS	RMSE	BIAS	RMSE	BIAS	RMSE	BIAS
Experiments														
CTRL	263.636	250.140	12.398	6.674	14.654	-13.373	0.017	-0.017	1.666	1.613	1.220	1.109	2.579	1.864
BDY_T2	249.395	240.660	12.383	6.253	14.116	-12.853	0.017	-0.017	1.912	1.817	1.275	1.162	2.943	1.307
BDY_T3	241.681	232.705	12.251	6.328	14.929	-13.737	0.017	-0.017	1.227	1.046	1.483	1.280	2.118	1.287
HFX_%75	151.119	134.594	12.544	6.354	14.740	-13.426	0.017	-0.017	3.078	3.016	0.956	0.826	3.335	0.874
HFX_%125	357.711	335.556	12.439	6.152	14.244	-13.043	0.017	-0.017	1.026	0.860	1.303	1.231	3.265	2.052
Noah	125.695	120.313	23.350	20.664	12.757	-11.502	0.048	0.048	1.046	0.983	10.116	9.904	2.788	1.795

566

567 Table 2. Summary of surface and air variables verification including integration hours from 3 to 12 h for Tazhong station.

568

**Reference:**

- Chen, F., and J. Dudhia, 2001a: Coupling an Advanced Land Surface–Hydrology Model with the Penn State–NCAR MM5 Modeling System. Part II: Preliminary Model Validation. *Monthly Weather Review*, **129**, 587–604.
- , 2001b: Coupling an advanced land surface-hydrology model with the Penn State–NCAR MM5 modeling system. Part I: Model implementation and sensitivity. *Monthly Weather Review*, **129**, 569–585.
- Dudhia, J., 1989: Numerical study of convection observed during the winter monsoon experiment using a mesoscale two-dimensional model. *J. Atmos. Sci.*, **46**, 3077–3107.
- Engelstaedter, S., R. Washington, C. Flamant, D. J. Parker, C. J. T. Allen, and M. C. Todd, 2015: The Saharan heat low and moisture transport pathways in the central Sahara—Multi-aircraft observations and Africa-LAM evaluation. *Journal of Geophysical Research: Atmospheres*, **120**, 2015JD023123.
- Garcia-Carreras, L., and Coauthors, 2015: The Turbulent Structure and Diurnal Growth of the Saharan Atmospheric Boundary Layer. *Journal of the Atmospheric Sciences*, **72**, 693–713.
- Han, B., S. Lü, and Y. Ao, 2012: Development of the convective boundary layer capping with a thick neutral layer in Badanjinlin: Observations and simulations. *Adv. Atmos. Sci.*, **29**, 177–192.
- Heinold, B., P. Knippertz, and J. H. Marsham, 2013: Large Eddy Simulations of Nocturnal Low-Level Jets over Desert Regions and Implications for Dust Emission. *EGU General Assembly Conference*.
- Heinold, B., P. Knippertz, and R. J. Beare, 2015: Idealized large-eddy simulations of nocturnal low-level jets over subtropical desert regions and implications for dust-generating winds. *Quarterly Journal of the Royal Meteorological Society*, **141**, 1740–1752.
- Heinze, R., D. Mironov, and S. Raasch, 2015: Second-moment budgets in cloud topped boundary layers: A large-eddy simulation study. *Journal of Advances in Modeling Earth Systems*, **7**, 510–536.
- Hong, S.-Y., and H.-L. Pan, 1996: Nonlocal boundary layer vertical diffusion in a medium-range forecast model. *Monthly weather review*, **124**, 2322–2339.
- Hong, S.-Y., and J.-O. J. Lim, 2006: The WRF single-moment 6-class microphysics scheme (WSM6). *J. Korean Meteor. Soc.*, **42**, 129–151.
- Hu, X.-M., J. W. Nielsen-Gammon, and F. Zhang, 2010: Evaluation of Three Planetary Boundary Layer Schemes in the WRF Model. *Journal of Applied Meteorology and Climatology*, **49**, 1831–1844.
- Kain, J. S., 1993: Convective parameterization for mesoscale models: The Kain-Fritsch scheme. *The representation of cumulus convection in numerical models*, *Meteor. Monogr*, **46**, 165–170.
- Kain, J. S., 2004: The Kain–Fritsch Convective Parameterization: An Update. *JOURNAL OF APPLIED METEOROLOGY*, **43**, 170–181.
- LeMone, M. A., M. Tewari, F. Chen, and J. Dudhia, 2013: Objectively Determined Fair-Weather CBL Depths in the ARW-WRF Model and Their Comparison to CASES-97 Observations. *Monthly Weather Review*, **141**, 30–54.
- Liu, Y., Q. He, H. Zhang, and A. Mamtimin, 2012: Improving the CoLM in Taklimakan Desert hinterland with accurate key parameters and an appropriate parameterization scheme. *Adv. Atmos. Sci.*, **29**, 381–390.
- Liu, Y., and Coauthors, 2011: Simultaneous nested modeling from the synoptic scale to the LES scale for wind energy applications. *Journal of Wind Engineering and Industrial Aerodynamics*, **99**,

- 613 308-319.
- 614 Marsham, J. H., P. Knippertz, N. Dixon, D. J. Parker, and G. M. S. Lister, 2011: The importance of the  
615 representation of deep convection for modeled dust - generating winds over West Africa during  
616 summer. *Geophysical Research Letters*, **38**.
- 617 Mlawer, E. J., S. J. Taubman, P. D. Brown, M. J. Iacono, and S. A. Clough, 1997: Radiative transfer for  
618 inhomogeneous atmospheres: RRTM, a validated correlated-k model for the longwave. *J. Geophys.*  
619 *Res.*, **102**, 16663-16682.
- 620 Moeng, C.-H., J. Dudhia, J. Klemp, and P. Sullivan, 2007: Examining Two-Way Grid Nesting for Large  
621 Eddy Simulation of the PBL Using the WRF Model. *Monthly Weather Review*, **135**, 2295-2311.
- 622 National Centers for Environmental Prediction, N. W. S. N. U. S. D. o. C., 2015: NCEP GDAS/FNL  
623 0.25 Degree Global Tropospheric Analyses and Forecast Grids. Research Data Archive at the  
624 National Center for Atmospheric Research, Computational and Information Systems Laboratory.
- 625 Rai, R. K., L. K. Berg, B. Kosović, J. D. Mirocha, M. S. Pekour, and W. J. Shaw, 2017: Comparison of  
626 Measured and Numerically Simulated Turbulence Statistics in a Convective Boundary Layer Over  
627 Complex Terrain. *Boundary-Layer Meteorology*, **163**, 69-89.
- 628 Schicker, I., D. Arnold Arias, and P. Seibert, 2016: Influences of updated land-use datasets on WRF  
629 simulations for two Austrian regions. *Meteorology and Atmospheric Physics*, **128**, 279-301.
- 630 Shin, H. H., and S. Y. Hong, 2011: Intercomparison of Planetary Boundary-Layer Parametrizations  
631 in the WRF Model for a Single Day from CASES-99. *Boundary-Layer Meteorology*, **139**, 261-281.
- 632 Shin, H. H., and S.-Y. Hong, 2015: Representation of the Subgrid-Scale Turbulent Transport in  
633 Convective Boundary Layers at Gray-Zone Resolutions. *Monthly Weather Review*, **143**, 250-271.
- 634 Skamarock, W. C., and Coauthors, 2008: A Description of the Advanced Research WRF Version 3. .  
635 *NCAR/TN-475+STR, NCAR TECHNICAL NOTE*.
- 636 Smirnova Tatiana, G., M. Brown John, G. Benjamin Stanley, and D. Kim, 2000: Parameterization of  
637 cold - season processes in the MAPS land - surface scheme. *Journal of Geophysical Research:*  
638 *Atmospheres*, **105**, 4077-4086.
- 639 Smirnova, T. G., J. M. Brown, and S. G. Benjamin, 1997: Performance of Different Soil Model  
640 Configurations in Simulating Ground Surface Temperature and Surface Fluxes. *Monthly Weather*  
641 *Review*, **125**, 1870-1884.
- 642 Stull, R. B., 1988: An Introduction to Boundary Layer Meteorology. *Atmospheric Sciences Library*, **8**,  
643 89.
- 644 Sun, J., and Q. Xu, 2009: Parameterization of Sheared Convective Entrainment in the First-Order  
645 Jump Model: Evaluation Through Large-Eddy Simulation. *Boundary-Layer Meteorology*, **132**,  
646 279-288.
- 647 Talbot, C., E. Bou-Zeid, and J. Smith, 2012: Nested Mesoscale Large-Eddy Simulations with WRF:  
648 Performance in Real Test Cases. *Journal of Hydrometeorology*, **13**, 1421-1441.
- 649 ter Maat, H. W., E. J. Moors, R. W. A. Hutjes, A. A. M. Holtslag, and A. J. Dolman, 2012: Exploring the  
650 Impact of Land Cover and Topography on Rainfall Maxima in the Netherlands. *Journal of*  
651 *Hydrometeorology*, **14**, 524-542.
- 652 WANG, and Coauthors, 2016a: Summer atmospheric boundary layer structure in the hinterland of  
653 Taklimakan Desert, China. *Journal of Arid Land*, **8**, 846-860.
- 654 Wang, M., X. Xu, and H. Xu: The possible influence of the summertime deep atmospheric boundary  
655 layer process over the Taklimakan Desert on the regional weather. (*submitted to Quarterly Journal*  
656 *of the Royal Meteorological Society*).

657 Wang, M. Z., H. Lu, H. Ming, and J. Zhang, 2016b: Vertical structure of summer clear-sky  
658 atmospheric boundary layer over the hinterland and southern margin of Taklamakan Desert: The  
659 deep convective boundary layer of Taklamakan Desert. *Meteorological Applications*, **23**, 438-447.  
660 Zhang, F., Z. Pu, and C. Wang, 2017: Effects of Boundary Layer Vertical Mixing on the Evolution of  
661 Hurricanes over Land. *Monthly Weather Review*, **145**, 2343-2361.  
662

For Review Only